August 2014

Master's Degree Thesis

Porcine epidemic diarrhea virus (PEDV) replication inhibitory coumarins from *Saposhnikovia divaricata*

Chosun University Graduate School

Department of Pharmacy

Basanta Dhodary

Porcine epidemic diarrhea virus (PEDV) replication inhibitory coumarins from *Saposhnikovia divaricata*

방풍으로부터 분리한 코마린계 화합물의 PEDV 복제 저해활성

2014 년 08 월 25 일

Chosun University Graduate School

Department of Pharmacy

Basanta Dhodary

Porcine epidemic diarrhea virus (PEDV) replication inhibitory coumarins from *Saposhnikovia divaricata*

지도교수 최홍석

공동 지도 교수 오 원 근

이 논문을 약학 석사학위신청 논문으로 제출함

2014년 04월

조선대학교 대학원

약학과

바산타 도다리

This thesis is examined and approved for

Basanta Dhodary's master degree

Chairman Chosun Univ. Prof. Choi Hoo Kyun (인)

Member Seoul National Univ. Prof. Kang Keon Wook (인)

Member Chosun Univ. Prof. Choi Hong Seok (인)

2014 년 05 월

Chosun University Graduate School

Contents

List of Schemes

List of Tables

List of Figures

List of Abbreviations

PED	porcine epidemic diarrhea
PEDV	porcine epidemic diarrhea virus
ORF	open reading frame
DMEM	dulbecco's modified eagle’s medium
DTT	dithiothreitol
FBS	fetal bovine serum
FT-IR	fourier transformed infrared
HMBC	heteronuclear multiple bond correlation
HMQC	heteronuclear multiple quantum coherence
HPLC	high performance liquid chromatography
HRFABMS	high resolution fast atom bombardment mass spectroscopy
IC_{50}	50% inhibitory concentration
IR	infrared
m/z	mass to charge ratio
MTT	3-(4, 5-dimethylthiazol-2-yl)-2, 5-diphenyl-tetrazolium bromide
NMR	nuclear magnetic resonance
OCC	open column chromatography
ppm	parts per million
RP	reverse phase
TLC	thin layer chromatography
UV	ultra violet
RNA	ribonucleic acid

SD	standard deviation
CPE	cytopathic effect
TGE	transmissible gastroenteritis
SARS-CoV	Severe acute respiratory syndrome – Coronavirus

(국문 초록)

방풍으로부터 분리한 코마린계 화합물의 PEDV 복제 저해활성

바산타 도다리

지도교수: 최홍석

공동지도교수: 오원근

약학과

조선대학교 대학원

돼지, 소, 닭 등의 축산을 기반으로 하는 축산산업은 prophylactic defense와 신뢰 있는 치료제의 부족으로 인한 porcine epidemic diarrhea virus (PEDV) 감염의 위험에 여전히 세계적으로 노출되어있다. PEDV 바이러스를 저해하는 생리활성을 측정하는 방법을 사용하여 *Saposnikovia divaricata* (방풍) 뿌리의 메탄올 추출물로부터 화합물을 분리한 결과, 3개의 새로운 coumarin glucosides 화합물인 divaricoumarin A (**1**), divaricoumarin B (**2**)와 divaricoumarin C (**3**) 및 기 구조가 확인된 2개의 코마린계 화합물 (**4-5**)를 얻을 수 있었다. 새로 분리된 화합물의 ^{1}H, ^{13}C-NMR, HMBC 및 HMQC등의 분광학적인 방법을 이용하여 화합물의 구조를 결정하였으며, 특히 신규화합물들의 절대적 구조결정을 위하여 ECD (electronic circular dichroism (ECD) 계산법을 사용하여 정확한 구조가 결정되었다.

방풍으로부터 분리한 모든 화합물 중, 이미 알려진 angular pyranocoumarin인

hyuganin C (**5**)는 PEDV 증식을 강하게 저해하는 효과가 측정 되었다. 정량적인 real-time PCR 결과는 PEDV 바이러스의 구조적 단백질인 nucleocapsid, GP2 spike 및 GP5 membrane 생합성을 담당하는 주요 유전자에 대한 화합물 **5**의 농도의존적인 의존적 저해효과를 보여주고 있다. 또한, western blotting 분석 결과는 PEDV nucleocapsid와 GP2 spike protein 생합성에 대한 명확한 저해효과를 보여주고 있다. 현재의 결과는 화합물 **5**가 가축의 PEDV 감염시 바이러스 증식 저해를 통한 치료약물로 효과적인 출발물질로서 사용 가능함을 제시하고 있다.

ABSTRACT

Porcine epidemic diarrhea virus (PEDV) replication inhibitory coumarins from *Saposhnikovia divaricata*

Basanta Dhodary

Advisor: Prof. Choi Hong Seok, Ph.D.

Co-Advisor: Prof. Oh Won Keun, Ph.D.

Department of Pharmacy,

Graduate School of Chosun University

Swine based agro-industries throughout the world are still in big threat of PEDV infection due to lack of efficient prophylactic defenses as well as dependable curing agents. Bioactivity-guided fractionation of methanol soluble extract from radix of *Saposnikovia divaricata* led to the isolation of three new coumarin glucosides, designated as divaricoumarin A (**1**), divaricoumarin B (**2**), divaricoumarin C (**3**), together with two known coumarins (**4**-**5**).Structures of the new isolates (**1**-**3**) were established by extensive spectroscopic analysis and absolute configurations were assigned based on ECD calculations. Among all isolates, the known angular pyranocoumarin, hyuganin C (**5**), revealed strong inhibitory effect on PEDV replication. Quantitative real-time PCR data showed inhibitory effect of **5** on gene responsible for PEDV vital structural protein synthesis (Nucleocapsid, GP2 spike, and GP5 membrane) in a dose-dependent manner. Also, it revealed the inhibitory effect on PEDV nucleocapsid and GP2 spike protein synthesis. The present result indicates the strong potentiality of compound **5** for curing PEDV infection via viral replication inhibition.

1. Introduction

1.1. Porcine Epidemic Diarrhea

Porcine epidemic diarrhea (PED) is a devastating infectious enteric disease of pigs; its sporadic outbreak in pig farms characterized by severe watery diarrhea leads for huge damage on pigs age-independently and can cause the death of young piglets.[1, 2] For the first time it was observed among English feeder and flattening pigs in the year 1971 and due to its rapid spreads throughout the Europe, it was named as ‘ epidemic viral diarrhea (EVD)’. However, in the year 1976 different type of EVD caused severe diarrhea in pigs of all ages and was classified as EVD type II, different from the previously recognized type I.[3] Finally, in 1978 it was recognized that EVD type II was turned out to be caused by a coronavirus-like agent and since that time the disease was named as ‘Porcine Epidemic Diarrhea”.[4, 5]

Porcine epidemic diarrhea is caused by an important pathogen, porcine epidemic diarrhea (PEDV), and clinical appearance is very similar to those of transmissible gastroenteritis (TGE) except that in certain outbreaks piglets under 4–5 weeks of age do not become sick.[6] Morbidity is variable in sow but high (approaching 98.7%) in suckling pigs, which are most severely affected and exhibit vomiting, watery diarrhea, and dehydration. Mortality in piglets may be 50% or higher. Most fattening pigs and weaners recover from the disease, but some may remain unthrifty. In adults, anorexia, lethargy, and diarrhea are seen, but mortality is very low. Comparing high morbidity, the mortality is usually low in adult pigs (3%), which can recover within in a week. However, when suckling pigs are involved, mortality is normally about 50% and can reach up to 90% in very severe outbreaks.[7]

PED was prevalent throughout European countries such as Germany, England,

Belgium, France, the Netherlands, and Switzerland during1980s and 1990s. After that, PED become a source of concern in Asia, where outbreaks are often more acute and severe with high than those observed in Europe. For example, Japanese outbreaks between September 1993 and June 1994 resulted in 14,000 deaths, with mortality ranging from 30 to 100% in suckling pigs.[8] PED outbreaks also occurred in Thailand from 2007 to 2008. Most of the affected farms reported that the disease first occurred in farrowing barns; 100% of newborn piglets were subsequently lost. Between August 1997 and July 1999, 50.4% of 1,258 enteric cases across 5 Korean provinces were diagnosed as PED.[9] Recently, at the end of January of 2014, the outbreak had occurred in 23 US states, where 2,692 confirmed cases caused severe economic losses.[10] Cumulatively, it suggests that the virus had become endemic in different areas at different time interval with huge monetary loss.

1.2. Porcine Epidemic diarrhea Virus

Porcine epidemic diarrhea virus (PEDV), the causative agent of porcine epidemic diarrhea, dehydration, vomiting, and high mortality in the piglets, is known for the family of Coronaviridae containing enveloped, single-stranded RNA.[4, 11, 12] PEDV ranges in diameter from 95 to 1990 nm (mean diameter: 130 nm), including its projection. As in many particles with a tendency to a round shape, the PEDV contains a centrally located electron-opaque body; it also possesses widely spaced club-shaped projections measuring 18–23 nm in length. The internal structure of the virus remains unknown. The virus possesses a glycosylated peplomer (spike, S) protein, Poll (P1), envelope (E), glycosylated membrane (M) protein, and an unglycosylated RNA-binding nucleocapsid (N) protein.

Virus Classification:

Group	:	Group IV **(**(+) ssRNA**)**
Order	:	Nidovirales
Family	:	Coronaviridae
Subfamily	:	Coronavirinae
Genus	:	Alphacoronavirus
Species	:	Porcine epidemic diarrhea virus

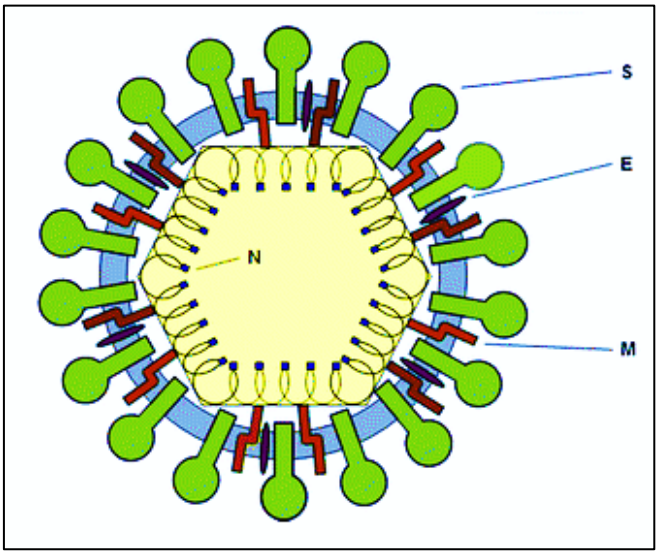

Fig. 1. Diagrammatic representation of PEDV

PEDV is an enveloped virus possessing an approximately 28 kb, positive-sense, single-stranded RNA genome with a 5′ cap and a 3′ polyadenylated tail.[12] The genome comprises a 5′ untranslated region (UTR), a 3′ UTR, and at least seven open reading frames (ORFs) that encode 4 structural proteins namely spike (S), envelope (E), membrane (M), and nucleocapsid (N) proteins and three non-structural proteins

(replicases 1a and 1b, and ORF3). The polymerase gene consists of two large ORFs, 1a and 1b that cover the 5′ two-third of the genome and encode the non-structural replicase polyproteins (replicases 1a and 1b). Genes for the major structural proteins S (150–220 kDa), E (7 kDa), M (20–30 kDa), and N (58 kDa) are located downstream of the polymerase gene.[13-15] The ORF3 gene, which is an accessory gene, is located between the structural genes and encodes an accessory protein, the number and sequence of which varies among different coronaviruses.[15]

The PEDV S protein is a type I glycoprotein composed of 1,383 amino acids. It contains a signal peptide, neutralising epitopes, a transmembrane domain, and a short cytoplasmic domain. The S protein can also be divided into S1 and S2 domains based on its homology with S proteins of other coronaviruses.[16-21] Like other coronavirus S proteins, the PEDV S protein is a glycoprotein peplomer (surface antigen) on the viral surface, where it plays a pivotal role in regulating interactions with specific host cell receptor glycoproteins to mediate viral entry, and stimulating induction of neutralising antibodies in the natural host.[13, 16-18, 21, 22] Moreover, it is associated with growth adaptation in vitro, and attenuation of virulence in vivo.[23, 24] Thus, the S glycoprotein has always been a primary target for the development of effective vaccines against PEDV.

The PEDV M protein, the most abundant envelope component, is a triple-spanning structural membrane glycoprotein with a short amino-terminal domain on the outside of the virus and a long carboxy-terminal domain on the inside.[25] The M protein not only plays an important role in the viral assembly process but also induces antibodies that neutralise the virus in the presence of its complement.[26-28] The M protein may play a role in α-interferon (α-IFN) induction.[29] Co-expression of M and E proteins allowed the formation of pseudoparticles, which exhibited interferogenic activity

similar to that of complete virions.[30]

The N protein, which binds to virion RNA and provides a structural basis for the helical nucleocapsid, is a basic phosphoprotein associated with the genome.[31, 32] As such, it can be used as the target for the accurate and early diagnosis of PEDV infection. It has been suggested that N protein epitopes may be important for induction of cell-mediated immunity.[28]

Even though the genes encoding the structural proteins have been thoroughly investigated for most coronaviruses, little is known about the functions of the accessory proteins, which are not generally required for virus replication in cultured cells.[32-35] In the case of PEDV, the only accessory gene is ORF3, which is thought to influence virulence; cell culture adaptation has been used to alter the ORF3 gene in order to reduce virulence.[36]

1.3. Diagnostic Tools for Porcine Epidemic diarrhea

A diagnosis of PED cannot be made on the basis of clinical signs and histopathological lesions.[37, 38] Due to the similarities in causative agents of diarrhoea, differential diagnosis is necessary to identify the PEDV in the laboratory.[38] Many techniques have been used for the detection of PEDV, including immunofluorescence tests, immunohistochemical techniques, direct electron microscopy, and enzyme-linked immunosorbent assays (ELISA). However, these techniques are time-consuming and are low in sensitivity and specificity.[39] When compared three techniques (RT-PCR, immunohistochemistry and in situ hybridization) for the detection of PEDV, RT-PCR identified the presence of PEDV more frequently than the other methods, but when only formalin-fixed tissues are submitted, immunohistochemistry and in situ hybridization would be useful methods for the detection of PEDV Ag and nucleic acid.[40]

1.4. Treatment Measures against PED

Several PEDV vaccines, which differ in their genomic sequence, mode of delivery, and efficacy, have been developed. As the disease caused by PEDV was not of sufficient economic importance to start the vaccine development in Europe, the trial of vaccine development was mainly accomplished in Asian countries where the PEDV outbreaks have been so severe that the mortality of the new born piglets was increased. In Japan, a commercial attenuated virus vaccine of cell culture-adapted PEDV (P-5V) has been administered to sows since 1997. Although these vaccines were considered efficacious, not all sows developed solid lactogenic immunity.[41]

Oral vaccination with attenuated PEDV DR13 has been proven to be more efficacious than injectable vaccine. Further, this vaccine candidate remained safe even after three back passages in piglets.[42] Piglet mortality can be reduced by orally inoculating pregnant sows with the DR13 strain. The viral strain was licensed, and used as an oral vaccine in South Korea from 2004. And the oral vaccine was registered and commercialized in Philippine at 2011. Despite the documented benefits of the DR13 vaccine, it does not significantly alter the duration of virus shedding—an indication of immune protection in challenged piglets.[43, 44]

1.5. Plant Coumarins

Coumarins owe their class name to 'Coumarou', the vernacular name of the tonka bean (*Dipteryx odorata* Willd., Fabaceae), from which coumarin itself was isolated in 1820.[45] Coumarin is classified as a member of the benzopyrone family of compounds, all of which consist of a benzene ring joined to a pyrone ring.[46] The benzopyrones can be subdivided into the benzo-α-pyrones to which the coumarins

belong and the benzo-γ-pyrones, of which the flavonoids are principal members.

There are four main coumarin sub-types namely the simple coumarins, furanocoumarins, pyranocoumarins and the pyrone-substituted coumarins. The simple coumarins are the hydroxylated, alkoxylated and alkylated derivatives of the parent compound, coumarin, along with their glycosides. Furanocoumarin consist of a five membered furan ring attached to the coumarin nucleus, divided into linear or angular types with substituent at one or both of the remaining benzoid positions. Pyranocoumarin members are analogous to furanocoumarins, but contain a six-membered ring. Coumarins substituted in the pyrone ring are the pyrone-substituted coumarins.

Coumarins possess a wide range of pharmacological properties including cytoprotective and modulatory functions, which may be translated into therapeutic potential for multiple diseases. Several natural and synthetic coumarins and derivatives, such as coumarin glycosides, possess potent biological activities. Coumarin derivatives are found in antibiotic, antimitotic, immunomodulating, antiviral, anticancer, anti-inflammatory, anticoagulant, antifungal, antioxidant, and cytotoxic agents, as well as some biological assays.[47] Coumarins have additional industrial applications. The fluorescence of coumarins, such as 7-hydroxycoumarin, is widely used as a research tool in polymer science. Coumarins are used as laser dye-sensitized photo initiators, for incorporation into polymer chains by co-polymerization, in the estimation of polymer solvent effects, for various structural characterizations, in the monitoring of the releasing properties of poly (methyl methacrylate) nanospheres and for polymeric fluorescent solar collectors.

1.6. *Saposhnikovia divaricata*

Saposhnikovia divaricata Schischk. (synonyms.: *Ledebouriella seseloides* WOLFF) belonging to the plant family Umbelliferae, is an important Chinese and Japanese traditional medicine, called Fang-feng and Bofu, respectively.[48] It is a perennial herb which is native to eastern Siberia and northern Asia. The herb is listed as a high-grade drug in the old Chinese Materia Medica, Shen Nung Pen Tsao Ching, and is applied for headaches, vertigo, generalized aching and arthralgia due to "wind, cold and dampness" in the traditional medical system.[49]

Fig. 2. *Saphosnikovia divaricata* (A) Whole plant; (B) Aerial part; (C) Sliced radix

Classification:

Kingdom : Plantae

Division : Magnoliophyta

Class : Magnoliopsida

Order : Apiales

Family : Apiaceae

Genus : *Saposhnikovia*

Species : *divaricata*

Based on the previous pharmacological experiments reported on the root extract, it shows suppressive nature on adjuvant arthritis, inhibitory effects on the CNS and peptic ulcers, and fegrifugal analgesic, anti-convulsant, anti-oxidant and anti-inflammatory activities, etc. Furthermore, several chemical studies on this herb had been done, and many components such as chromones, coumarins, lignans, sterols and polyacetylenes were isolated.[48] Even though, several phytochemical screenings had been carried out and evidences were available to support it as a popular ingredient in the formula for preventing and treating people who are prone to catching cold as well as bacterial and viral swine disease in traditional Chinese medicine, till now there is no any reported evidence on the specific antiviral activity with elucidated chemical entities.

In this study, bioactivity-guided fractionation of EtOAc soluble fraction by subjecting to silica gel and reverse phase silica gel column chromatographic techniques and HPLC, yielded three new coumarin glycosides, divaricoumarin A (**1**), divaricoumarin B (**2**) and divaricoumarin C (**3**) together with two known pyranocoumarins namely *cis*-khellactone (**4**)[50, 51] and hyuganin C (**5**).[52]

2. Materials and Methods

2.1. Materials

2.1.1. Plant material

The dried radixes of *S. divaricate* were purchased from a market in Gwangju, South Korea, in February 2011 and were identified botanically by Prof. Won Keun Oh, College of Pharmacy, Seoul National University, Seoul, South Korea. A voucher specimen (CU2011-05) has been deposited at the Laboratory of Pharmacognosy, College of Pharmacy, Seoul National University.

2.1.2. Chemicals, reagents and chromatography

Open column chromatography was conducted on silica gel (63-200 and 40-63 μm particle size) and RP-18 (40-63 μm particle size) from Merck. TLC was carried out with silica gel 60 F_{254} and RP-18 F_{254} plates from Merck. HPLC was carried out using a Gilson system with a UV detector and Optima Pak C_{18} column (10×250 mm, 10μm particle size, RS Tech, Korea). HPLC solvents MeOH and MeCN were purchased from B&J (Burdick & Jackson®, USA). Deuterated solvents $CDCl_3$ and acetone were purchased from CIL (Cambridge Isotope Lab., USA) for NMR analysis.

Azauridine was purchased from Sigma Chemical Company (St Louis, MO, USA). Dulbecco's modified Eagle's medium (DMEM), fetal bovine serum (FBS), and trypsin were purchased from GIBCO-BRL (Grand Island, NY, USA). MTT [3-(4, 5-dimethylthiazol-2-yl)-2, 5-diphenyltetrazolium bromide] was purchased from Sigma, Korea.

2.1.3. General experimental procedures

Optical rotations were determined on a Rudolph Autopol IV polarimeter using a 100 mm glass microcell. IR spectra (KBr) were recorded on a Nicolet 6700 FT-IR (Thermo Electron Corp.). The 1D and 2D NMR spectra (^{1}H and ^{13}C NMR, NOESY, HSQC and HMBC) were performed using a Varian Unity Inova 500 MHz spectrometer with TMS as the internal standard. HR-FABMS data were obtained with JEOL JMS-700 mass spectrometer. Silica gel (Merck, 63-200μm and 40-63 μm particle size), RP-18 (Merck, 40−63μm particle size) were used for column chromatography. TLC was carried out with silica gel 60 F_{254} and RP-18 F_{254} plates. HPLC was carried out using Gilson HPLC system with 321 pump and UV/VIS-155 detector. Optima Pak C_{18} column (10×250 mm, 10μm particle size, RS Tech, Korea) was used as HPLC column. All solvents used for extraction and isolation were of analytical grade.

2.2. Methods

2.2.1. Extraction and isolation

The dried radixes of *S. divaricate* (8.0 kg) were extracted with MeOH (3 x 15 L) at room temperature for 1 week. The combined MeOH extract was concentrated to yield the dry residue (1.80 kg). Then, the crude extract was suspended in H_2O (3 L) and partitioned successively with *n*-hexane (3 × 2 L), EtOAc (3 × 2 L), and *n*-BuOH (3 × 2 L). The bioactive EtOAc-soluble extract (72.0 g) was chromatographed over a silica gel column (10 x 40 cm; 63-200 μm particle size) by eluting with *n*-hexane-Acetone gradient (20:1 to 0:1) to afford seven fractions (F1-F7). Fraction F2 - F5 were found to be active against PEDV. Fraction F2 (9g) was subjected to reverse phase open column chromatography (RP-18) with mobile phase MeOH:H_2O (1:1 to 1:0) and fractionated to

seven sub-fractions (F2.1 to F2.7). Then the sub-fraction F2.3 (1.4g) was further purified using Gilson HPLC system [RS Tech Optimapak C18 column (10 × 250 mm, 10 μm particle size); eluted with 75% methanol in water with flow rate 2 mL/min; UV-detection at 205 and 254 nm] leading to the isolation of Compound **4** (12mg). Fraction F3 yielded three compounds **5** (36 mg) upon chromatographic fractionation using RP-18 (MeOH:H_2O- 1:2 to 1:0) subsequently applying the sub-fraction 3.1 to the RP18 open column (MeOH:H_2O- 1:4 to 1:0) and finally purifying the sub-fraction 3.1.4 using HPLC [RS Tech Optimapak C-18 column (10 × 250 mm, 10 μm particle size; flow rate of 2mL/min; UV-detection at 205 and 254 nm)] with 50% MeOH in water. Fraction F5 (14 g) was purified by a silica gel column chromatography eluted with a gradient of *n*-hexane-Acetone (7:1 to 0:1). Subfraction F5.4 (4.7 g) was further purified by an RP-18 column eluting with a stepwise gradient of MeOH:H_2O (1:3 to 1:0) to afford six subfractions (F5.4.1-F5.4.6). The subfraction F5.4.2 (0.8 g) was subjected to Optima Pak C18 column [(10 × 250 mm, 10 μm particle size, RS Tech, Korea); mobile phase CH_3CN in H_2O containing 0.1% HCO_2H (0-60 min: 30% CH_3CN, 60-70 min: 100% CH_3CN); flow rate 2 mL/min; UV detection at 205 and 254 nm] to give compounds **1** (58.0 mg), **2** (20.0 mg) and **3** (4.0 mg).

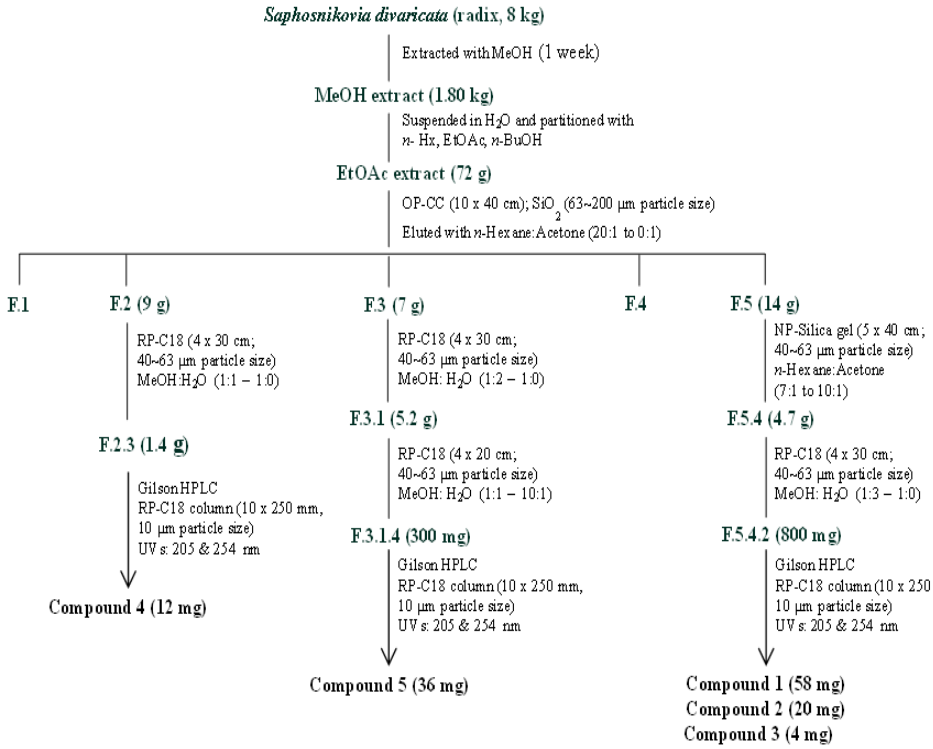

Scheme 1. Isolation of new compounds (**1**–**3**) from *S. divaricata*

Divaricoumarin A (1)

Brownish, powder; $[\alpha]_D^{25}$ +23.0 (*c* 0.2, MeOH); UV (MeOH) λ_{max} nm (log ε) 200 (sh, 3.19), 318 (2.19); ECD (MeOH, Δε) 217 (-3.90), 252 (+2.89), 299 (-9.87); IR (KBR) ν_{max} 3390, 2955, 1734, 1615, 1460, 1250, 1014 cm^{-1}; ^1H (500 MHz, acetone-d_6) and ^{13}C (125 MHz, acetone-d_6) NMR data, see Table 1; HRFABMS *m/z* 525.1983 $[M + H]^+$ (calcd for $C_{25}H_{33}O_{12}$, 525.1972).

Compound 1a:

White powder; ECD (MeOH, Δε) 225 (+4.25), 252 (+0.91), 289 (-1.06), 329 (+0.43); ^1H NMR (600 MHz, acetone-d_6) δ 7.89 (1H, d, *J* = 9.60 Hz, H-4), 7.53 (1H, d,

J = 8.20 Hz, H-5), 6.73 (1H, d, *J* = 8.20 Hz, H-6), 6.17 (1H, d, *J* = 9.60 Hz, H-3), 5.89 (1H, s, H-1'), 1.34 (3H, s, H-5'), 1.32 (3H, s, H-4'); HRTOFMS *m/z* 277.0742 $[M - H]^-$ (calcd for $C_{14}H_{13}O_6$, 277.0712).

Divaricoumarin B (2):

Brownish, powder; $[\alpha]_D^{25}$ +34.0 (*c* 0.2, MeOH); UV (MeOH) λ_{max} nm (log ε) 202 (sh, 3.22), 222 (3.09), 318 (2.83); ECD (MeOH, Δε) 223 (-4.0), 249 (+3.97), 299 (-12.61); IR (KBR) ν_{max} 3387, 2945, 1721, 1609, 1448, 1246, 1026 cm^{-1}; ^1H (500 MHz, acetone-d_6) and ^{13}C (125 MHz, acetone-d_6) NMR data, see Table 1; HRFABMS *m/z* 523.1814 $[M + H]^+$ (calcd for $C_{25}H_{31}O_{12}$, 523.1816).

Divaricoumarin C (3):

Brownish, powder; $[\alpha]_D^{25}$ +47.0 (*c* 0.2, MeOH); UV (MeOH) λ_{max} nm (log ε) 202 (sh, 2.97), 222 (2.79), 318 (2.49); ECD (MeOH, Δε) 214 (+1.05), 228 (-7.66), 296 (+0.73), 320 (-1.70); IR (KBR) ν_{max} 3383, 2941, 1724, 1603, 1452, 1242, 1023 cm^{-1}; ^1H (500 MHz, acetone-d_6) and ^{13}C (125 MHz, acetone-d_6) NMR data, see Table 1; HRFABMS *m/z* 523.1799 $[M + H]^+$ (calcd for $C_{25}H_{31}O_{12}$, 523.1816).

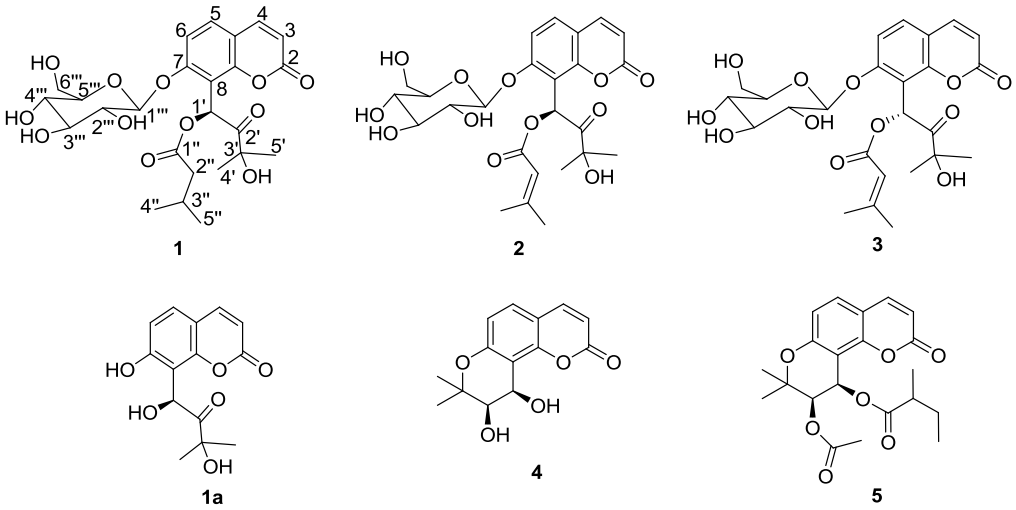

Fig. 3. Chemical structures of compounds **1**-**5** isolated from *S. divaricata*

2.2.2. Acid hydrolysis of compound 1

A solution of compound **1** (9.0 mg) in water was treated with 5% HCL and heated on a water bath maintained at 50 ^{o}C for 24 hours. After confirmation of the reaction completion (monitored by TLC), the resultant sample solution was partitioned with EtOAc. The EtOAc layer residue was analyzed by LC-MS system and based on mass analysis we isolated the aglycone of **1** in minor amount (0.2 mg) where as we were able to get **1a** in sufficient amout (0.7 mg) to proceed for further experiment to determine absolute configuration.

2.2.3. Computational Chemistry for ECD Calculation

Turbomole at the basis set def-SV(P) for all atoms and the functional B3LYP was used for the ground-state geometries optimization with density functional theory (DFT) calculations. Harmonic frequency calculation was used for the further confirmation of the ground states. The calculated ECD data corresonding to the optimized structures were obtained with TDDFT at the B3LYP functional. The ECD spectra were simulated by overlapping Gaussian functions for each transition (σ is the width of the band at *1/e* height). ΔE_i and R_i are the excitation energies and rotatory strengths for transition i, respectively. For this report, the value of σ was 0.10 eV.

$$\Delta\varepsilon(E) = \frac{1}{2.297 \times 10^{-39}} \frac{1}{\sqrt{2\pi\sigma}} \sum_{i}^{A} \Delta E_i \, R_i e^{[-(E-\Delta E_i)^2/(2\sigma)^2]}$$

2.2.4. Cell Culture and Virus Stock

Vero cells (African green monkey kidney cell line; ATCC CCR-81) were provided by American Type Culture Collection (ATCC, Manassas, VA, USA) and

maintained in Dulbecco's Modified Eagle's Medium (DMEM) supplemented with 10% fetal bovine serum (FBS), 100 U/mL penicillin and 100 μg/mL streptomycin. PEDV (porcine epidemic diarrhea virus) was obtained from Choong Ang Vaccine Laboratory, Korea. Virus stock was stored at −80 ℃ until use.

2.2.5. Cytotoxicity Assay

The cell viability was assessed using a MTT (3-(4,5-dimethyl-2-thiazolyl)-2,5-diphenyl-2H-tetrazolium bromide MTT methylthiazolyldiphenyl-tetrazolium bromide) based cytotoxicity assay. Vero cells were grown in 96-well plates at 1×10^5 cells per well and allowed to adhere for 24 hour prior to treatment. The cells in 96-well plates were treated with various concentrations of compounds and incubated for 48 hr. The final concentration of DMSO in the culture medium was maintained at 0.05% (v/v) to avoid solvent toxicity. Subsequently, 20 μL of the 2 mg/mL MTT solution was added to each well of the plate and incubated 4 hr. After removal of supernatant, 100 μL DMSO was added for solubilization of formazan crystals. Then the absorbance was measured at 550 nm. The percentage cell viability is expressed as toxicities of the compounds, where the higher the toxicity, the lower the cell viability. Percentage cell viability is defined as the absorbance in the experiment well compared to that in the control wells. Each experiment was carried out in triplicates. The 50% cytotoxic concentration (CC_{50}) was calculated by regression analysis.

2.2.6. Cytopathic Effect (CPE) Inhibition Assay

Vero cells were seeded onto 96-well culture plates at 1×10^5 cells per well. Next day, medium was removed and then washed with phosphate buffered saline (PBS). PEDV at 0.01 MOI was inoculated onto near confluent Vero cell monolayers for 2 hr.

The media was removed and replaced by DMEM with several compounds at different concentrations. Each concentration of compounds was determined in triplicate. The cultures were incubated for 3 days at 37 ℃ under 5% CO_2 atmosphere. Then, cells replaced with only DMEM and 20 μL of the 2 mg/mL MTT to each well and incubated at 37 ℃ for 4 hr. After that, next steps were followed cytotoxicity assay and the 50% effective concentration (EC_{50}) was calculated by regression analysis. A selective index (SI) was determined using the formula SI = CC_{50}/EC_{50}.

2.2.7. Quantitative Real-time PCR

Vero cells were grown to about 90% confluence in 6-well plates, infected with PEDV at 0.01 MOI and incubated for 2 hr. Then, media was removed and replaced by DMEM and cultured in the presence of various concentrations of compounds. After 24 hr, total RNA was isolated from the cells following TRIzol method. The total RNA was reverse transcribed using random primer (iNtRON Biotechnology, INC, Korea) according to manufacturer′s instruction. Real-time PCR was performed using selective primers for PEDV, which was listed in S-Table 1 (Supporting Information) and conducted using 2 μL of cDNA and Maxima SYBR Green qPCR master mix 2X (Thermo sci., Rockford, IL, USA). Cycling conditions for real-time PCR were follows: 95 ℃ for 10 min, followed by 40 cycles of 95 ℃ for 15 s, 60 ℃ for 1 min. Real-time PCR was conducted using the Step one Plus Real-time PCR system. The data was analyzed with StepOne software v2.3 (Applied Biosystems).

2.2.8. Western blot analysis

The cultures were prepared similar methods with quantitative Real-time PCR. After 24 hr, the cells were washed with cold PBS and stored at −80 ℃. For whole cell

lysate, the cells were lysed on ice in 100 μL lysis buffer [50 mM Tris-HCl (pH 7.6), 120 mM NaCl, 1 mM EDTA, 0.5% NP-40, 50 mM NaF] and centrifuged at 12,000 rpm for 20 min. Supernatants were collected from the lysates and protein concentrations were determined using protein assay kit (Bio-Rad Laboratories, Inc. USA). Aliquots of lysates were boiled for 5 min and electrophoresed on 10% or 12% SDS-polyacrylamide gels. Protein in the gels were electrotransferred to nitrocellulose membranes (PVDF 0.45 μm, Immobilon-P, USA). Membranes were then incubated with primary antibodies spike (S) protein, Nucelocapsid (N) (Abfrontier, Korea) or mouse monoclonal actin antibody. The membranes were further incubated with secondary antibodies. Finally, they were detected using enhanced chemiluminescence Western blottong dectection kit (Thermo sci., Rockford, IL, USA).

2.2.9. Immunofluorescence Assay

Vero cells were grown on 8-well chamber slides (LAB-TEK, NUNC, USA) and the cell monolayers were injected with PEDV at 0.01 MOI for 2 hr. The solution was removed and replaced by DMEM, and treated with the compounds at the corresponding concentration. The cultures were incubated for 24 hr at 37 ℃ under 5% CO_2 atmosphere. The cells were washed three times with PBS (pH 7.4) and fixed with a 4% paraformaldehyde solution for 30 min at room temperature. After blocking with 1% BSA for 1 hr, the cells were incubated overnight with monoclonal antibody against N protein of PEDV (Abfrontier, Korea) diluted 1:50 in PBS (pH 7.4). After washing with PBS (pH 7.4), the cells were incubated with FITC-conjugated goat anti-mouse lgG antibody (Jackson, ImmunoResearch, Inc.) for 1 hr. After washing three times with PBS (pH 7.4), the cells were stained with 500 nM DAPI solution for 10 min at room temperature and washed 3 times with PBS (pH 8.0). Slides were mounted with

mounting reagent for fluorescence (Vectashield, Vector Lab, Inc.) and observed by fluorescence microscopy (Olympus ix70 Fluorescence Microscope, USA).

2.2.10. Statistical Analysis

The results are expressed as the means ± SD of three independent experiments. Statistical analysis was performed using SigmaPlot® (version 11.0) software. Differences between group mean values were determined by one-way analysis of variance followed by a two-tailed Student's *t*-test for unpaired samples, assuming equal variances. Statistical significance was accepted at $p < 0.05$.

3. Results and Discussions

3.1. Structural determination of new compounds 1-3

Bioassay-guided fractionation of an EtOAc soluble extract of *Saposnikovia divaricata* radix led to the isolation of five coumarins, consisting of three new coumarin glucosides (**1**-**3**), together with two known coumarins (Fig. 3). The known compounds were identified as *cis*-khellactone and hyuganin C on the basis of spectroscopic analysis, chemical evidence and comparison with spectral data with those reported in the literatures.

3.1.1. Structural determination of compound 1

Compound **1** was isolated as brownish powder with positive optical rotation ($[\alpha]_D^{25}$= +23.0 in MeOH). Its molecular formula was assigned as $C_{25}H_{32}O_{12}$ based on the **[M + H]** $^+$ ion peak at *m*/*z* 525.1983 (calcd 525.1972) in the HRFABMS. In the ^{1}H NMR spectrum (Table 1), a pair of protons at δ_H 6.25 (d, *J* = 9.5 Hz) and 7.90 (d, *J* = 9.5 Hz) were assigned as H-3 and H-4, respectively, based on the HMBC correlations from characteristic C-2 at δ_C 160.1. From the NOESY spectrum, H-4 showed correlations to a proton at δ_H 7.65 (d, *J* = 8.7 Hz), indicating this proton being H-5. Consequently, the proton at δ_H 7.22 (d, *J* = 8.7 Hz) should be H-6. The absence of other coumarin protons in the ^{1}H NMR spectrum suggested the presence of a 7- and 8-substituted coumarin nucleus. In the HMBC spectrum, H-4 and H-5 showed correlations to two quaternary carbons at δ_C 115.1 and 154.0 ppm, indicating these carbons being C-10 and C-9, respectively. Also, H-5 (δ_H 7.65, d, *J* = 8.7 Hz) and H-6 (δ_H 7.22, d, *J* = 8.7 Hz) showed HMBC correlations to a quaternary carbon at δ_C 159.6, implying this carbon being C-7.

Thus, the last benzene carbon at δ_C 113.5 was determined as C-8. Furthermore, the HMBC correlation from the anomeric proton at δ_H 5.03 (d, J = 6.9 Hz) to C-7 (δ_C 159.6) and the coupling constant (J = 6.9 Hz) of the anomeric proton indicated the linkage of a β-D-glucopyranosyl moiety at C-7. The unusual singlet at δ_H 7.23 revealed the presence of an O-benzylic esterified methine. Moreover, the detailed analysis of ^{1}H and ^{13}C NMR data (Table 1) suggested the presence of isovaleryl group, which was further confirmed by the HMBC correlations from H-2'' (δ_H 2.23) to C-3'' (δ_C 26.5), from H-2'' (δ_H 2.23) and H-3'' (δ_H 2.08) to C-1'' (δ_C 172.4), from H-4''/5'' (6H, δ_H 0.93) to C-2'' (δ_C 43.6) and C-3'' (δ_C 26.5). The HMBC correlation from H-1' (δ_H 7.23) to C-1'' (δ_C 172.4) determined the linkage of this isovaleryl group at C-1'. The remaining part of structure was elucidated from the HMBC correlations from H-1' (δ_H 7.23), H_3-5' (δ_H 1.35), and H_3-4' (δ_H 1.25) to C-2' (δ_C 209.4), and H_3-5' (δ_H 1.35) and H_3-4' (δ_H 1.25) to C-3' (δ_C 77.3). Finally, the planar structure of compound **1** was constructed by the HMBC correlations from H-1' (δ_H 7.23) to C-7 (δ_C 159.6), C-8 (δ_C 113.5), and C-9 (δ_C 154.0), indicating the linkage of C-8 and C-1'. Thus, the structure of compound **1** was established as divaricoumarin A.

Divaricoumarin A (**1**) as a new isolate bears an asymmetric carbon center at C-1'. Firstly, we attempted to determine the absolute configuration with respect to that carbon center by using electronic circular dichroism (ECD) calculations based on time-dependent density functional theory. However, we found the same calculated ECD profile for 1'S- and 1'R- divaricoumarin A possibly due to the hindrance by intramolecular hydrogen bonding persisting between the sugar unit and isovaleryl substituent group. Next, we attempted to resolve the problem by acid hydrolysis and get aglycon of **1** and **1a**. Again, we try to determine the absolute configuration of compound **1a** at C-1' by ECD calculations utilizing time-dependent density functional theory. The

ECD profiles of 1'S and 1'R of compound **1a** are shown in Fig. 11. Interestingly, experimental CD profile of **1a** with negative Cotton effect at 289 nm, positive Cotton effects at 252 nm and 225 nm almost matched with **1a** (**S**), suggesting the assignment of 1'S configuration for **1a**. Furthermore, we can observe the similarity of experimental CD profile between **1a** and aglycon of **1** suggesting for the conservation of same configuration even though ester group get hydrolyzed from the structure by acid hydrolysis (Fig. 12). Hence, we can conclude that **1** also has the 1'S configuration. So far as we know, we are reporting the absolute configuration of this type of coumarin glycoside for the first time in this report.

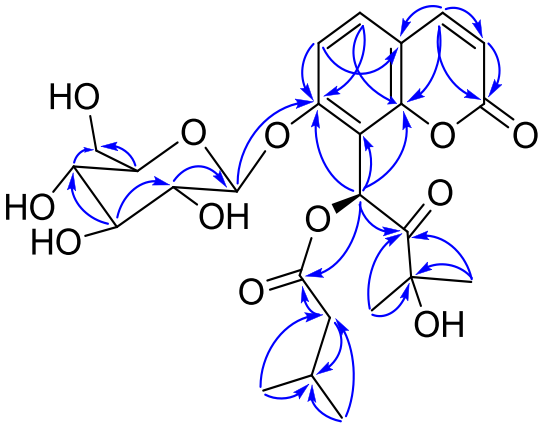

Fig. 4. Key HMBC (H→C) correlations of compound **1**

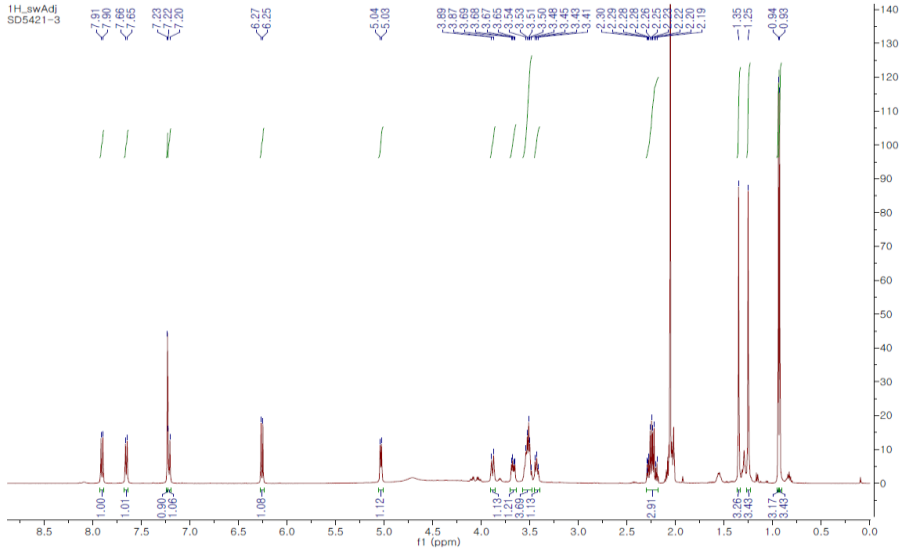

Fig. 5. ^{1}H-NMR (Acetone-d_6, 500 MHz) spectrum of compound **1**

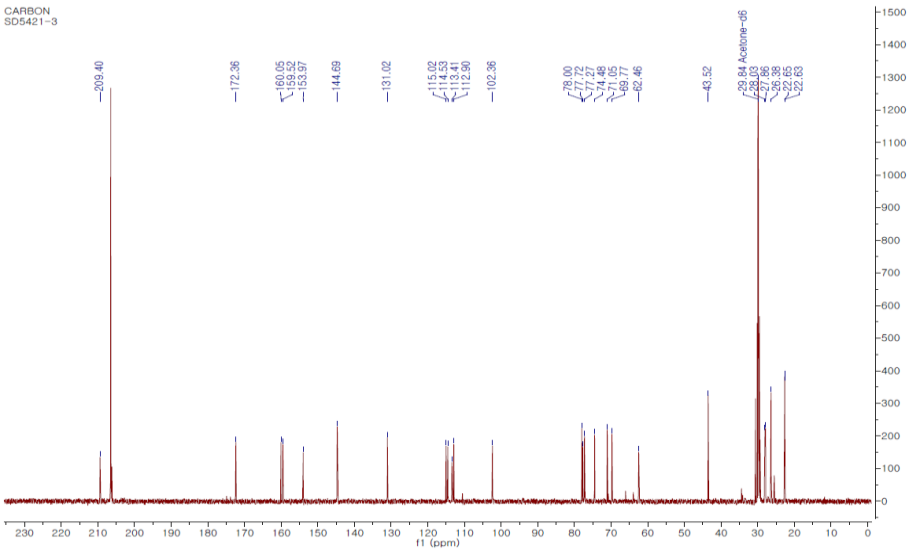

Fig. 6. ^{13}C-NMR (Acetone-d_6, 125 MHz) spectrum of compound **1**

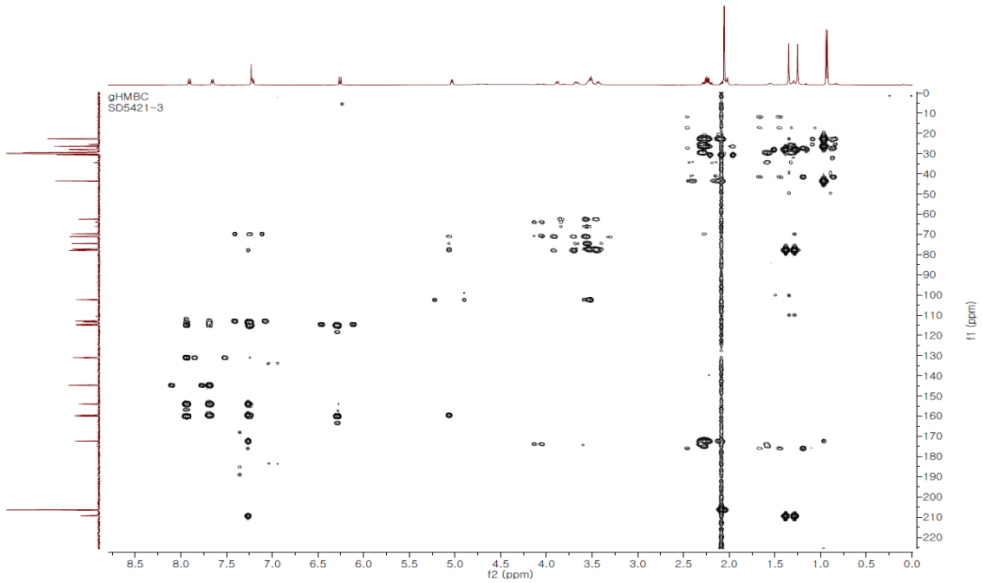

Fig. 7. HMBC spectrum of compound **1**

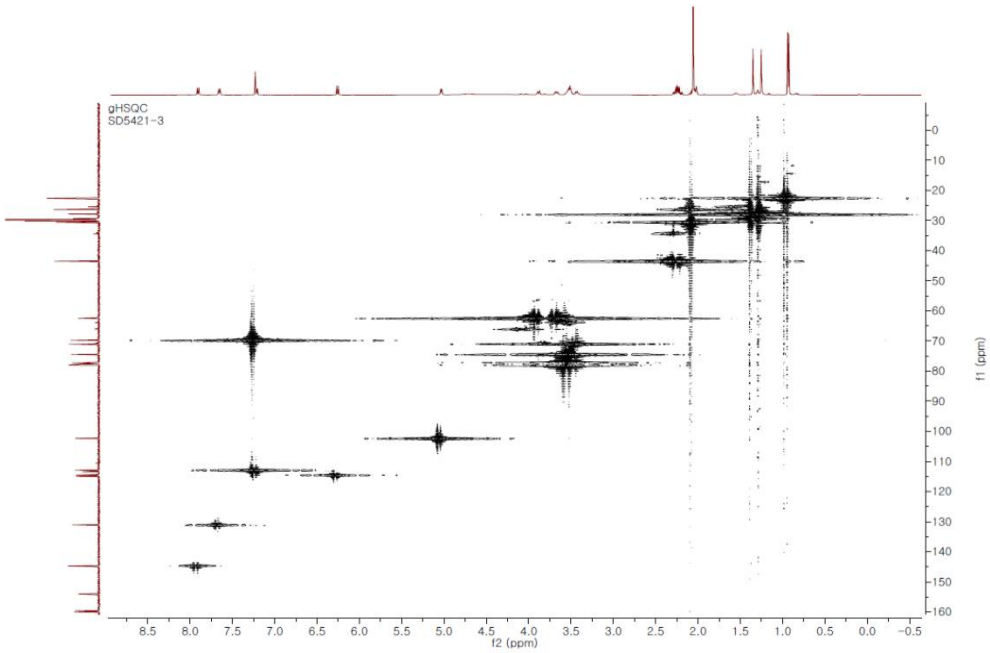

Fig. 8. HSQC spectrum of compound **1**

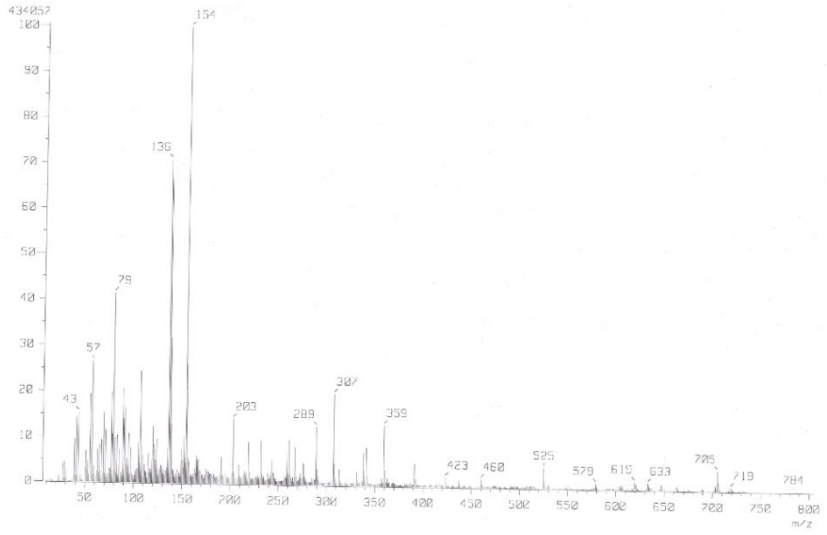

Fig. 9. FABMS spectrum of compound **1**

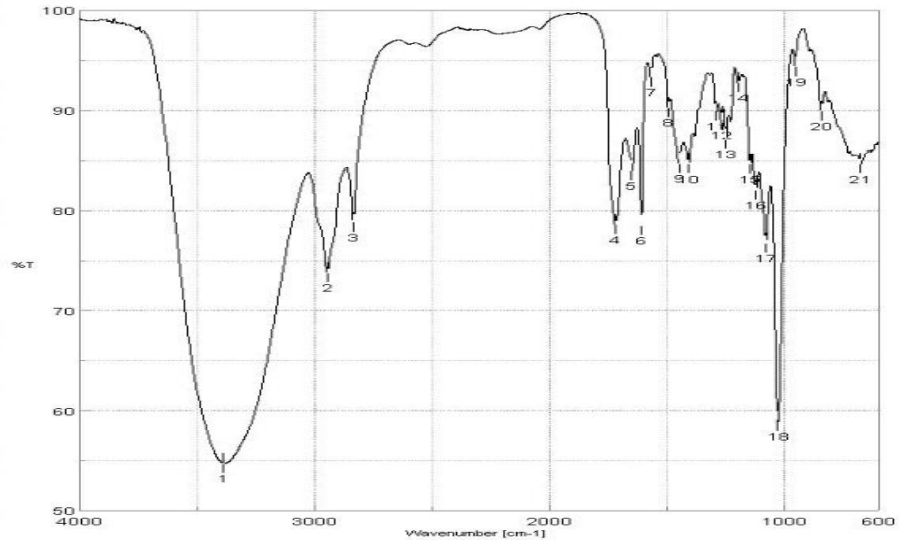

Fig. 10. IR (KBr) spectrum of compound **1**

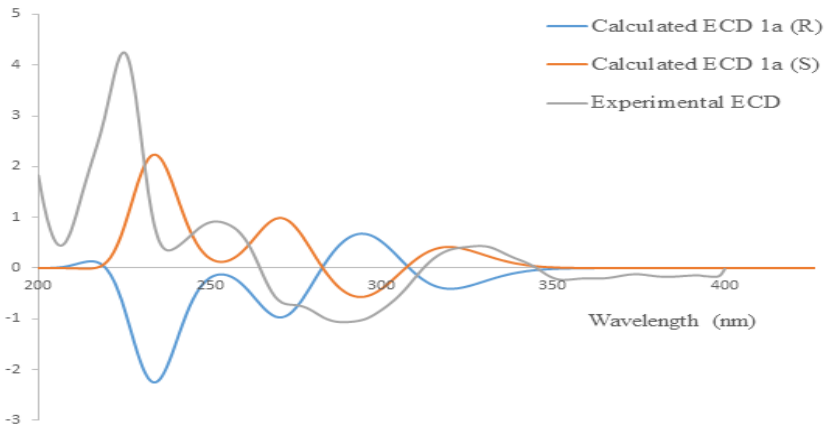

Fig. 11. Experimental ECD (in MeOH) and calculated ECD (**R**, **S**) spectra of compound **1a**

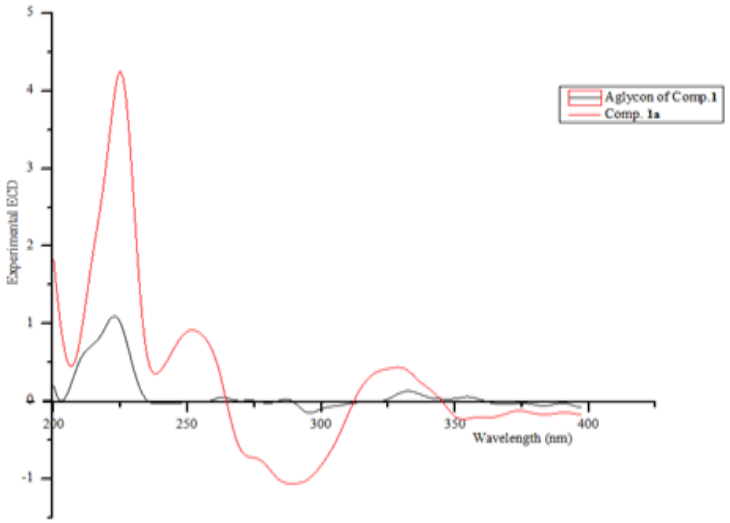

Fig. 12. Experimental ECD (in MeOH) spectra of aglycon of compound **1** and **1a**

3.1.2. Structural determination of compound 2

Compound **2** was isolated as brownish powder with positive optical rotation ($[\alpha]_D^{25}$= +34.0 in MeOH). Its molecular formula was assigned as $C_{25}H_{30}O_{12}$ based on the **[M + H]**$^+$ ion peak at *m*/*z* 523.1814 (calcd 523.1816) in the HRFABMS. As like the compound **1**, protons at δ_H 6.29 (H-3, d, *J* = 9.5 Hz), 7.94 (H-4, d, *J* = 9.5 Hz), 7.68 (H-5, d, *J* = 8.7 Hz) and 7.25 (H-6, d, *J* = 8.7 Hz) suggested the presence of a 7- and 8-substituted coumarin nucleus. The HMBC correlation from the anomeric proton at δ_H 5.06 (d, *J* = 6.0 Hz) to C-7 (δ_C 159.56) and the coupling constant (*J* = 6.0 Hz) of the anomeric proton indicated the linkage of a *β*-D-glucopyranosyl moiety at C-7. The unusual singlet at δ_H 7.35 revealed the presence of an O-benzylic esterified methine. Moreover, the detailed analysis of ^{1}H and ^{13}C NMR data (Table 1) suggested the presence of senecioyl group instead of isovaleryl group as compared to compound **1**, which was further confirmed by the HMBC correlations from H-2'' (δ_H 5.76) to C-3'' (δ_C 158.93), from H-2'' (δ_H 5.76) to C-1'' (δ_C 165.85), from H-4''/5'' (6H, δ_H 2.16 & δ_H 1.9) to C-2'' (δ_C 116.14) and C-3'' (δ_C 158.93). The HMBC correlation from H-1' (δ_H 7.35) to C-1'' (δ_C 165.85) determined the linkage of this senecioyl group at C-1'. The remaining part of the structure was elucidated with the help of HMBC correlations from H-1' (δ_H 7.35), H_3-5' (δ_H 1.39), and H_3-4' (δ_H 1.29) to C-2' (δ_C 209.55), and H_3-5' (δ_H 1.39) and H_3-4' (δ_H 1.29) to C-3' (δ_C 77.7). The structure of compound **2** was established as divaricoumarin B. Interestingly, we can see the similarity of experimental CD profiles between 1'S-divaricoumarin A (**1**) and **2** with a prominent negative Cotton effect at 299 nm, a positive Cotton effect at 249 nm and a negative Cotton effect at 223 nm, as shown in Figure 19. Finally, based on that similarity we can strongly suggest for the assignment of 1'S configuration for **2**.

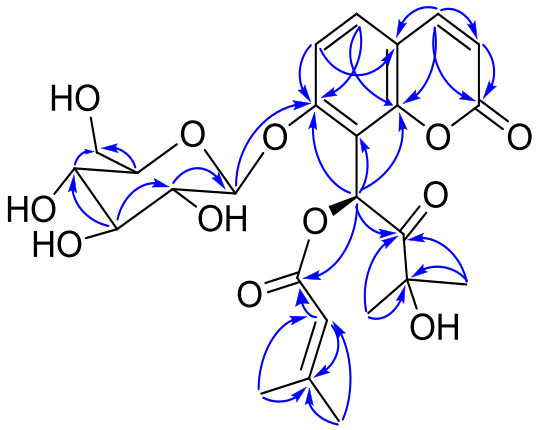

Fig. 13. Key HMBC (H→C) correlations of compound **2**

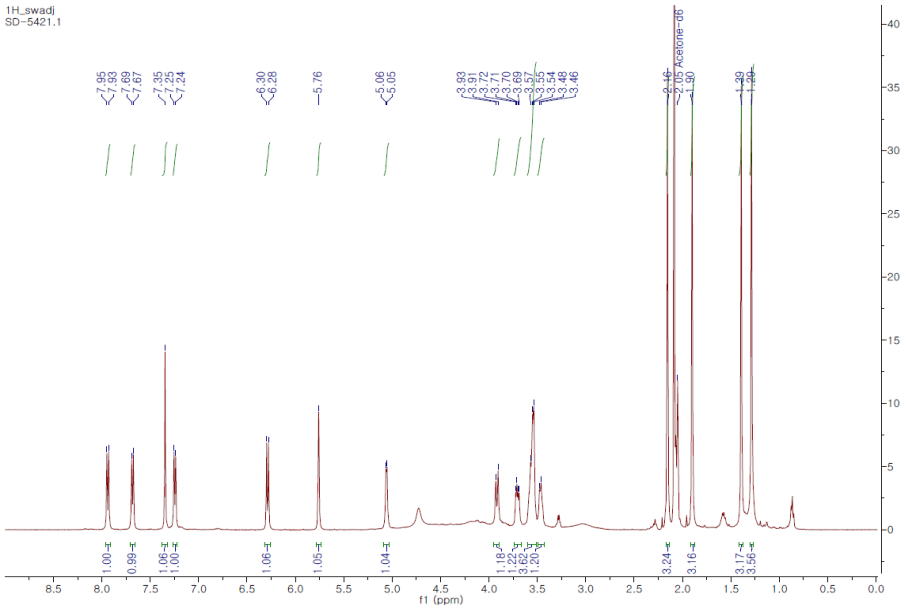

Fig. 14. ^{1}H-NMR (Acetone-d_6, 500 MHz) spectrum of compound **2**

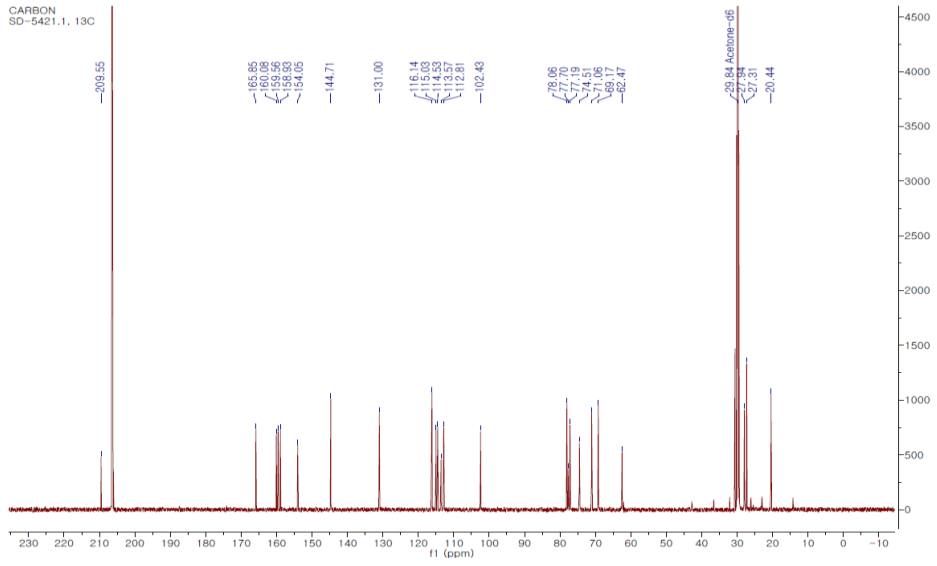

Fig. 15. ^{13}C-NMR (Acetone-d_6, 125 MHz) spectrum of compound **2**

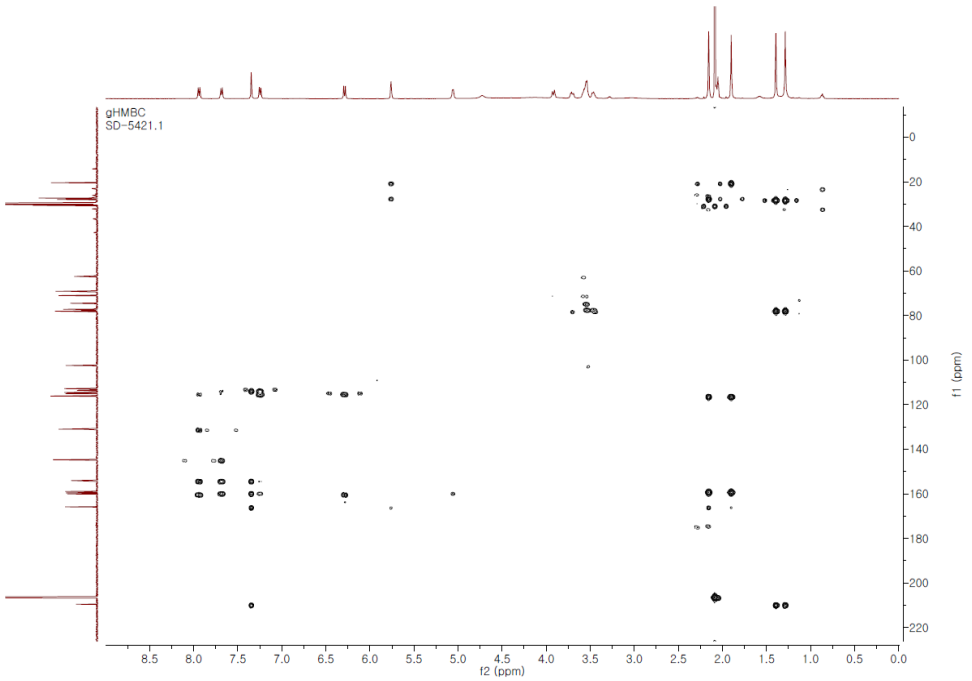

Fig. 16. HMBC spectrum of compound **2**

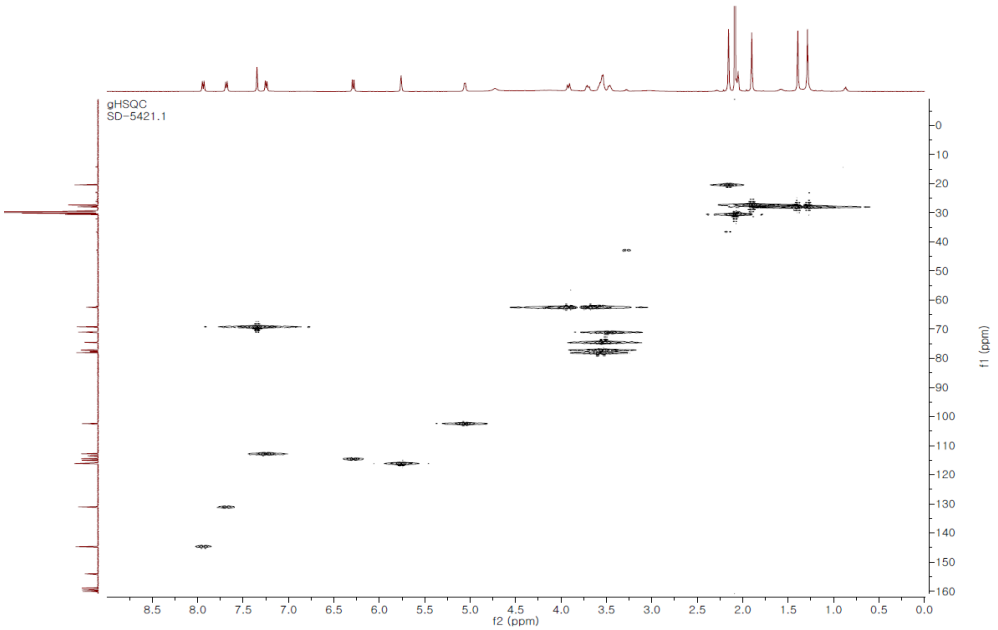

Fig. 17. HSQC spectrum of compound **2**

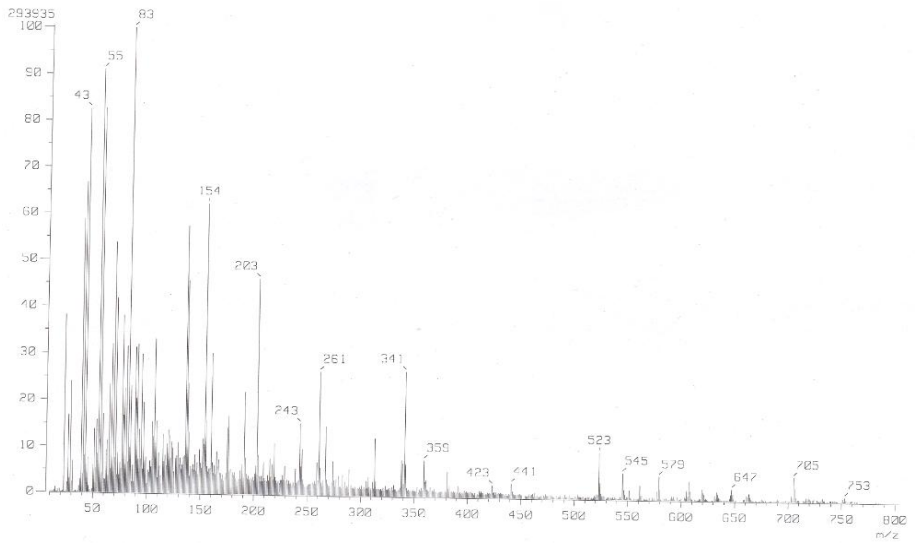

Fig. 18. FABMS spectrum of compound **2**

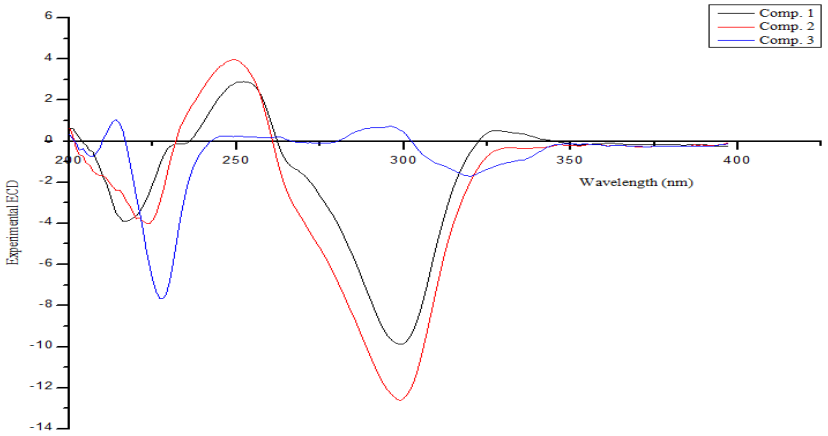

Fig. 19. Experimental ECD (in MeOH) spectra of compound **1**, **2** and **3**

3.1.3. Structural determination of compound 3

Compound **3** was isolated as brownish power with positive optical rotation ($[\alpha]_D^{25}$= +47.0 in MeOH). Its molecular formula was assigned as $C_{25}H_{30}O_{12}$ based on the **[M + H]**$^+$ ion peak at *m*/*z* 523.1799 (calcd 523.1816) in the HRFABMS. The ^{1}H and ^{13}C NMR data showed that compound **3** and compound **2** contain same number of carbon and proton signals with similar chemical shift values. But, in the ^{1}H NMR spectrum chemical shift of H-6 seems to be slightly different, at around δ_H 7.38 for compound **3** whereas for compound **2,** little up field, at around δ_H 7.25 (Table 1). Just like the compound **2,** it also reveals the presence of a 7- and 8-substituted coumarin nucleus, a *β*-D-glucopyranosyl moiety at C-7, an unusual singlet peak at δ_H 7.33 and senecioyl group at C-1' . However, when we compared the experimental CD profile with compound **2**, we can observe the dramatic difference with a positive Cotton effect at 320 nm and a prominent negative Cotton effect at 230 nm as shown in Figure 2C. As we already confirmed the absolute configuration for **2** as 1'S, compound **3** must be the

stereoisomer of **2** with 1'R configuration. Hence, the structure of compound **3** was established as divaricoumarin C.

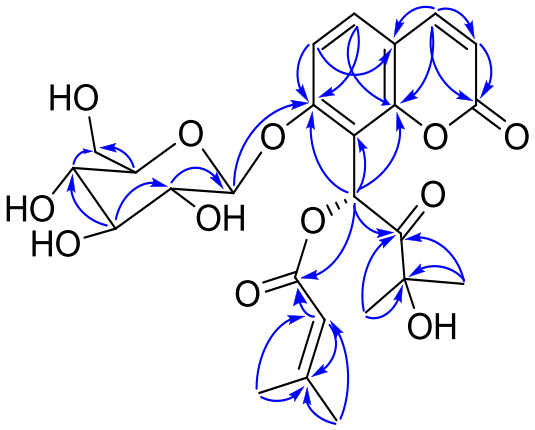

Fig. 20. Key HMBC (H→C) correlations of compound **3**

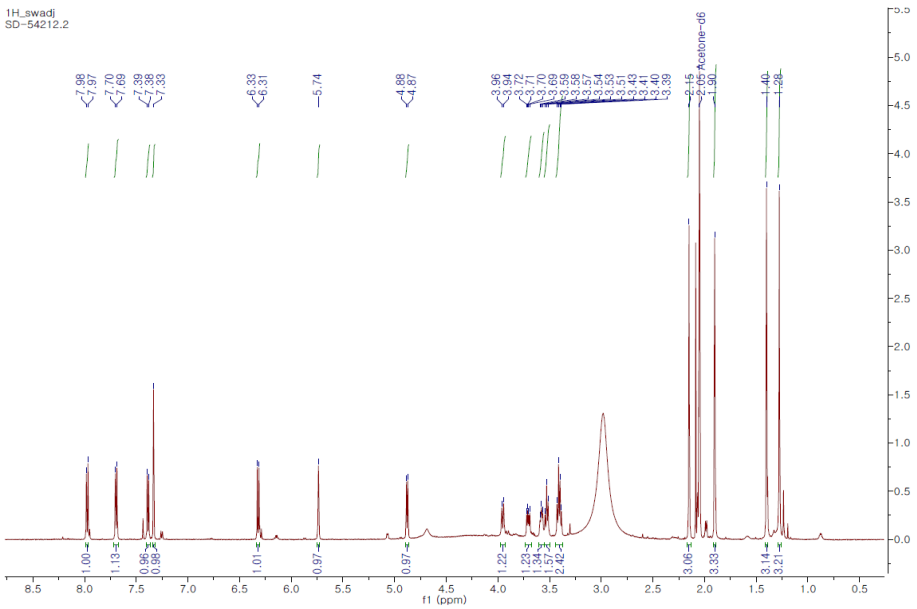

Fig. 21. ^{1}H-NMR (Acetone-d_6, 500 MHz) spectrum of compound **3**

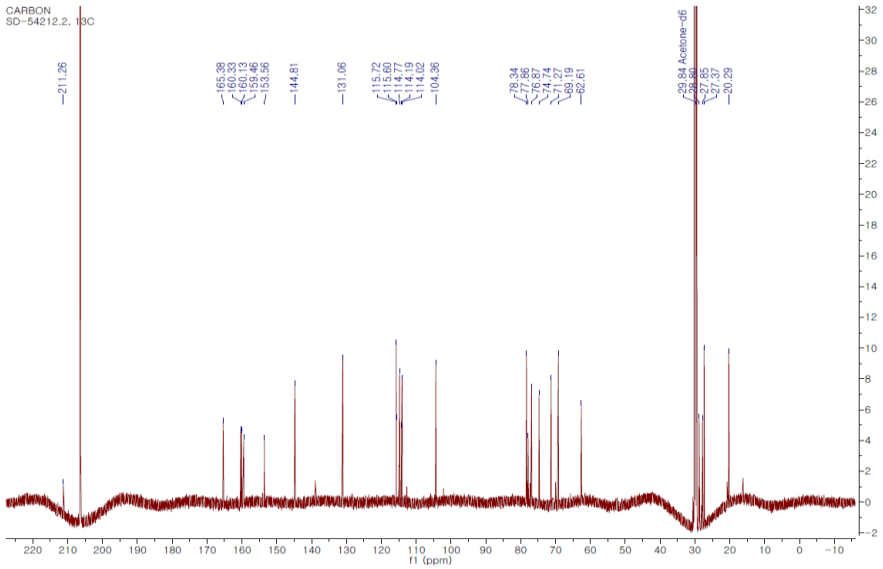

Fig. 22. ^{13}C-NMR (Acetone-d_6, 125 MHz) spectrum of compound **3**

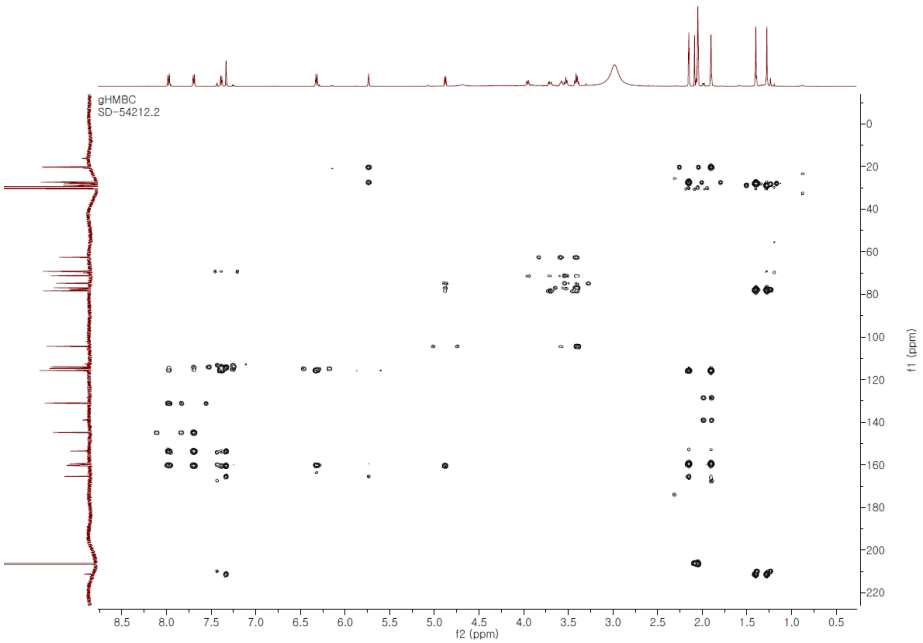

Fig. 23. HMBC spectrum of compound **3**

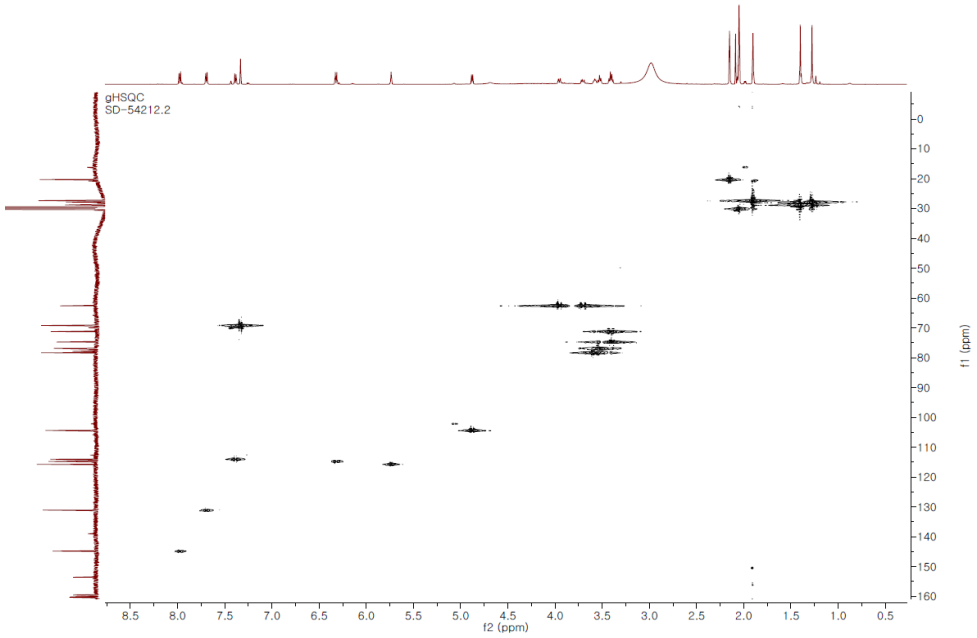

Fig. 24. HSQC spectrum of compound **3**

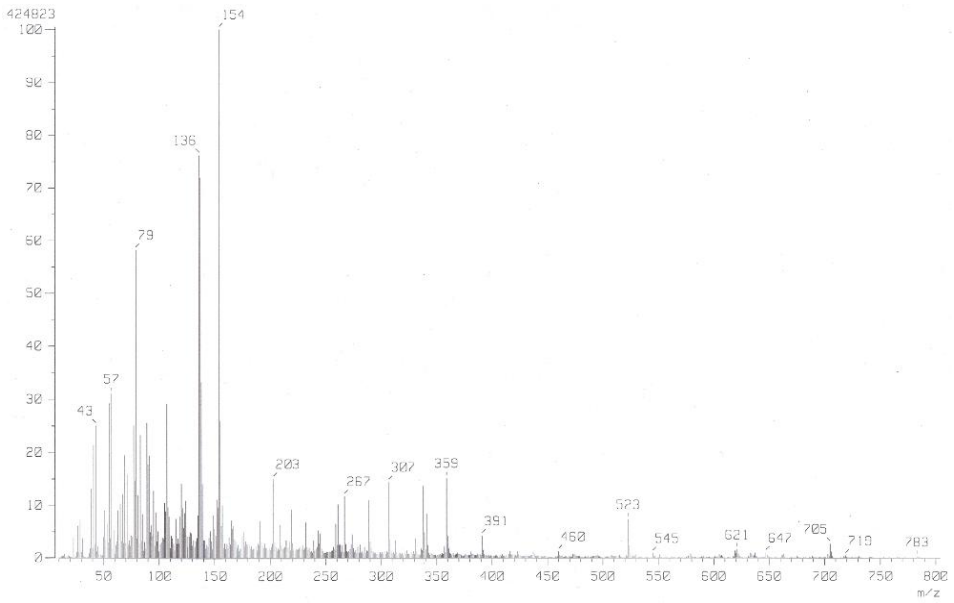

Fig. 25. FABMS spectrum of compound **2**

position	1[a]		2[a]		3[a]	
	δ_H (J in Hz)	δ_C	δ_H (J in Hz)	δ_C	δ_H (J in Hz)	δ_C
Aglycone						
2		160.1		160.08		160.1
3	6.25,d,9.5	114.6	6.29,d,9.5	114.53	6.32,d,9.5	114.7
4	7.9,d,9.5	144.8	7.94,d,9.5	144.71	7.98,d,9.5	144.7
5	7.65,d,8.7	131.1	7.68,d,8.7	131	7.69,d,8.7	130.9
6	7.22,d,8.7	112.9	7.25,d,8.7	112.81	7.38,d,8.7	113.9
7		159.6		159.56		160.3
8		113.5		113.57		114.1
9		154		154.05		153.5
10		115.1		115.03		115.5
1’	7.23,s	69.9	7.35,s	69.17	7.33,s	69.1
2’		209.4		209.55		211.2
3’		77.8		77.7		77.8
4’	1.25,s	27.9	1.29,s	27.94	1.28,s	27.8
5’	1.35,s	28.1	1.39,s	27.94	1.39,s	28.7
1”		172.4		165.85		165.3
2”	2.23,m	43.6	5.76,s	116.14	5.74,s	115.6
3”	2.08,m	26.5		158.93		159.4
4”	0.93,d,6.7	22.7	2.16,s	20.44	2.15,s	20.2
5”	0.93,d,6.7	22.7	1.9,s	27.31	1.9,s	27.3
Glucose						
1”’	5.03,d,6.9	102.4	5.06,d,6.0	102.43	4.88,d,7.7	104.3
2”’	overlap	74.6	overlap	74.51	overlap	74.7
3”’	overlap	77.3	overlap	77.19	3.51,m	76.8
4”’	3.44,m	71.1	3.47,d,8	71.06	overlap	71.2
5”’	overlap	78.1	overlap	78.06	3.55,m	78.3
6”’	3.88,br d,11.8 3.67,dd,11.8, 6	62.5	3.92,br d,11.6 3.71,dd,11.6, 5.8	62.47	3.95,br d,12 3.71,dd,12,6.2	62.5

Table 1. ^{1}H (500 MHz) and ^{13}C (125 MHz) -NMR data (in acetone-d_6) for compounds **1**, **2** and **3**

3.2. Anti-PEDV effect of isolated compounds

3.2.1. Assessment of PEDV inhibition via CPE Analysis

All coumarin isolates were evaluated for their inhibitory activity against PEDV through CPE analysis in Vero cells (Table 2). Of the compounds tested the known angular pyrano coumarins hyuganin C (**5**) and *cis*-khellactone (**4**) exhibited potent activity with EC_{50} values 5.91 ± 0.38 μM and 15.26 ± 0.67 μM, respectively. Interestingly, the most potent compound **5** showed almost similar activity as compared to positive control with safety index more than 8. In the other hand, new coumarin glucosides **1-3** revealed the moderate inhibitory activity against PEDV in dose dependent manner without any cytotoxicity (Fig. 26)

Table 2. Inhibitory effect of known coumarins **4-5** on PEDV induced CPE

Compound	CC_{50} (μM)	EC_{50} (μM)	SI
4	> 50	15.26 ± 0.67	> 3.50
5	> 50	5.91 ± 0.38	> 8.40
Azauridine	48.16 ± 5.14	3.36 ± 0.71	14.30 ± 1.24

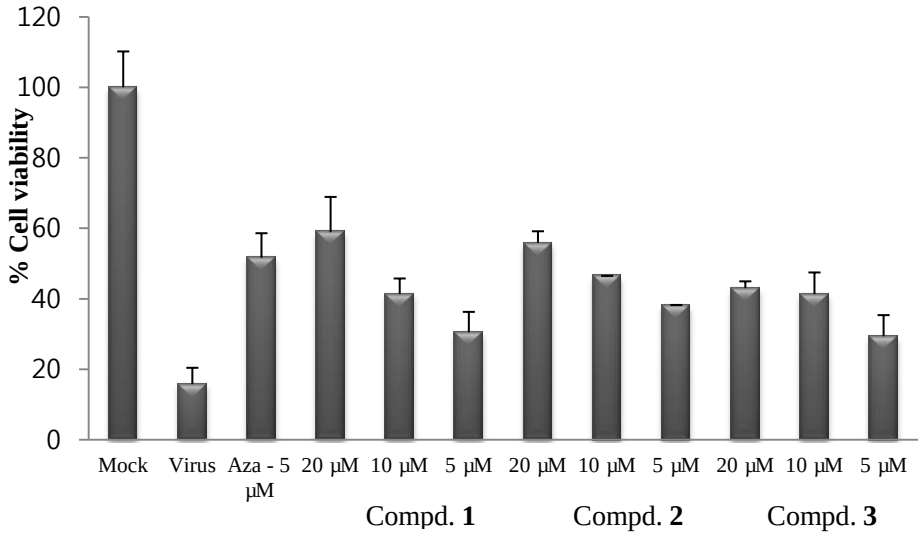

Fig. 26. Dose-dependent inhibitory effect of new compounds **1-3** on PEDV induced CPE

3.2.2. Assessment of PEDV replication inhibition

The stages like viral entry; viral penetrations in to the host cells, viral processing, viral replication and viral release from the infected cells in PEDV life cycle are the potential targets for the possible antiviral compounds.[27] During viral replication, genes encoding the viral structural proteins [nucleocapsid (N), membrane (M) and Spike (S)] are key elements for viral integrity.[28] To investigate the inhibitory effect of compound **5** on viral replication, quantitative real-time RT-PCR was performed using specific primers for viral nucleocapsid, GP2 spike and GP5 membrane encoding genes. Interestingly, quantitative real-time PCR analysis suggest that our most potent compound **5** exhibited inhibitory effect on genes encoding PEDV nucleocapsid, GP2

spike, and GP5 membrane proteins in a dose-dependent manner (Fig. 27). Compound **5** inhibitory effects were found to be better than positive control, azauridine, for all three structural proteins encoding genes at the same concentration of 10 μM. Moreover, western blot analysis supports for compound **5** dose-dependent inhibitory effects on viral nucleocapsid and GP2 spike protein synthesis (Fig. 28). The nucleocapsid and GP2 spike proteins representative level measured clearly indicated the compound **5**'s better inhibitory tendency towards both structural protein syntheses than positive control at same concentration. Furthermore, analysis of PEDV replication using an immunofluorescence assay revealed green fluorescence in virus-infected cells, but not in mock infected Vero cells. However, the treatment of cells with different concentration of compound **5** reduced the fluorescence-positive, PEDV infected cells in a dose-dependent manner (Fig. 29).

A

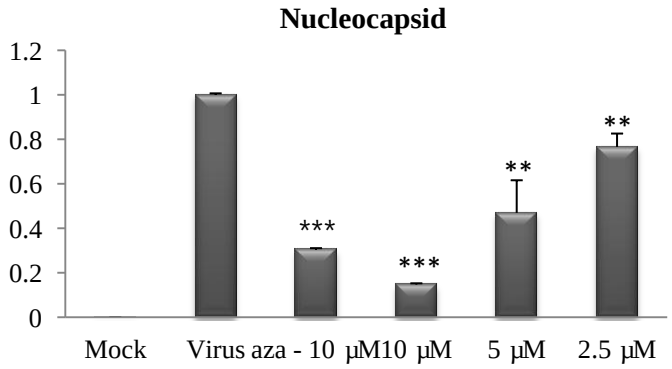

B

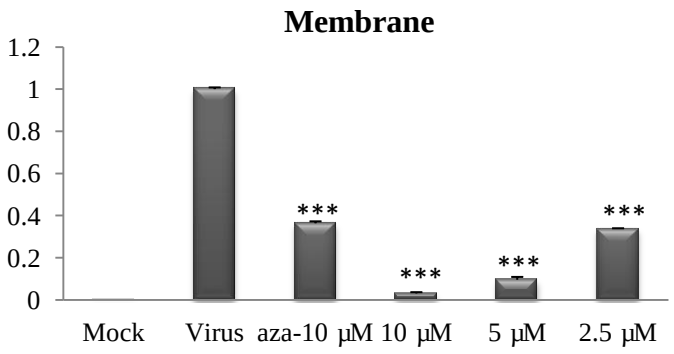

C

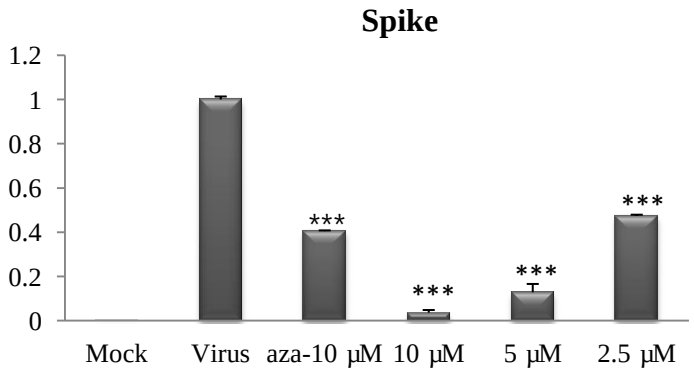

Fig. 27. Quantitative real-time PCR analysis revealing the inhibitory effect of compound **5** on gene encoding viral structural proteins. (A) Dose-dependent inhibitory effect of compound **5** on gene encoding nucleocapsid protein. (B) Dose-dependent inhibitory effect of compound **5** on gene encoding membrane protein. (C) Dose-dependent inhibitory effect of compound **5** on gene encoding spike protein.

A

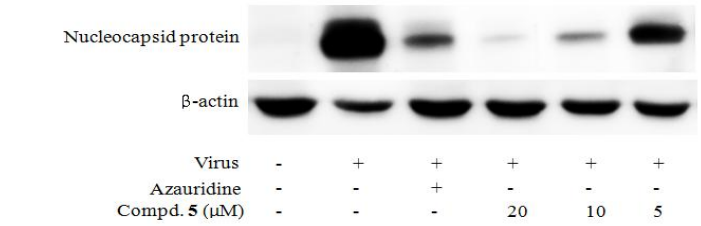

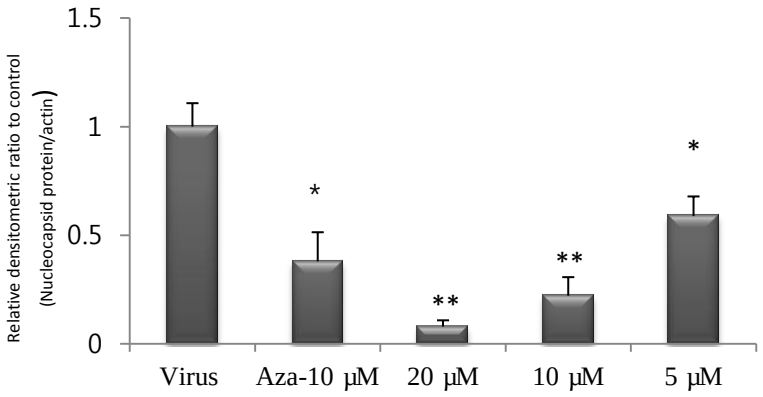

B

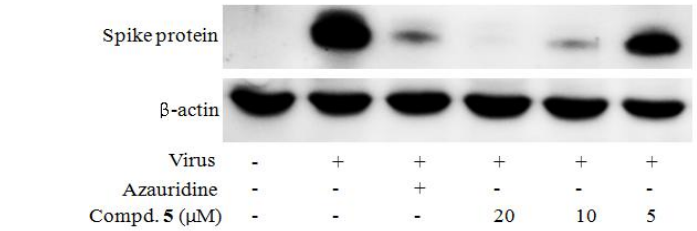

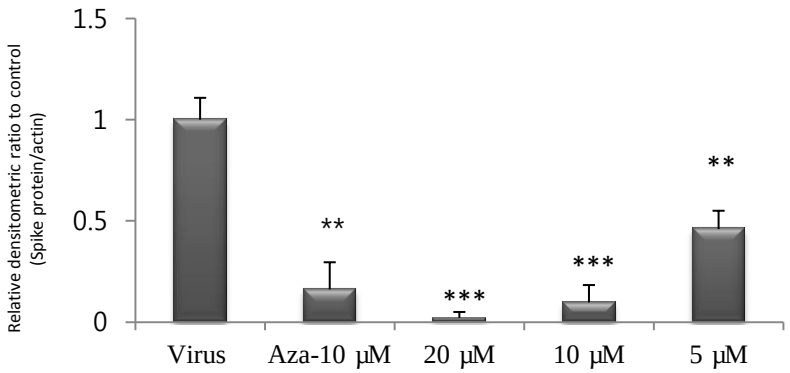

Fig. 28. Western blot analysis revealing the inhibitory effect of compound **5** on viral structural proteins synthesis. (A) Dose-dependent nucleocapsid protein synthesis inhibitory effect of compound **5**. (B) Dose-dependent spike protein synthesis inhibitory effect of compound **5**.

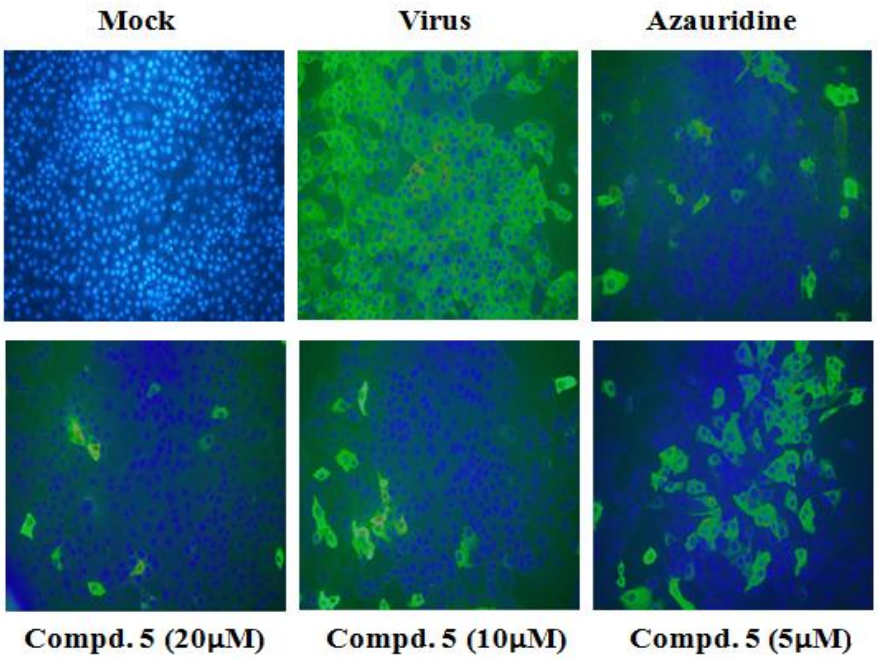

Fig. 29. Immunofluorescence image revealing the inhibition of PEDV replication by compound **5** in dose dependent manner.

4. Conclusions

Porcine epidemic diarrhea has been a serious issue in swine based agro-economy. This study has shown that coumarins from *S. divaricata* exert anti-PEDV effect by inhibiting viral replication in host cell. More clearly, Compound **5** showed strong inhibitory effect on viral nucleocapsid, GP2 spike and GP5 membrane encoding genes and their respective proteins. Based on the above findings, it can be suggested that coumarins from *S. divaricata* might be considered as viable antiviral lead candidates against PEDV infection.

Human corona viruses like SARS from same coronaviridae family shares some similar replication mechanism with PEDV. Previously quercetin type flavonoids from natural product origin has been reported for their potent inhibitory effect against PEDV and were also been reported for showing potent inhibitory effect against other type fatal human corona viruses like severe acute respiratory syndrome (SARS). Likewise, the coumarin molecules showing anti-PEDV effect in this report could also be the noteworthy candidates for further investigation against the fatal human coronaviruses.

5. References

1. Cho, W. K.; Kim, H.; Choi, Y. J.; Yim, N. H.; Yang, H. J.; Ma, J. Y., Epimedium koreanum Nakai Water Extract Exhibits Antiviral Activity against Porcine Epidermic Diarrhea Virus In Vitro and In Vivo. *Evid Based Complement Alternat Med* **2012,** 985151, (10), 29.
2. Song, D.; Park, B., Porcine epidemic diarrhoea virus: a comprehensive review of molecular epidemiology, diagnosis, and vaccines. *Virus Genes* **2012,** 44, (2), 167-75.
3. Wood, E. N., An apparently new syndrome of porcine epidemic diarrhoea. *Vet Rec* **1977,** 100, (12), 243-4.
4. Debouck, P.; Pensaert, M., Experimental infection of pigs with a new porcine enteric coronavirus, CV 777. *Am J Vet Res* **1980,** 41, (2), 219-23.
5. M.B. Pensaert; P. Callebaut; Bouck, P. d., Present knowledge. Int. Congr. . *Pig Vet. Soc.* **1982,** 52.
6. Hou, X.-L.; Yu, L.-Y.; Liu, J., Development and evaluation of enzyme-linked immunosorbent assay based on recombinant nucleocapsid protein for detection of porcine epidemic diarrhea (PEDV) antibodies. *Veterinary Microbiology* **2007,** 123, (1–3), 86-92.
7. B.E. Straw; S.D. Allaire; W.L. Mengeling; (Eds.), D. J. T., Diseases of Swine *Iowa State University Press, Iowa, EEUU* **1999**, 179–185.
8. Grundmann, F.; Kaiser, M.; Schiell, M.; Batzer, A.; Kurz, M.; Thanwisai, A.; Chantratita, N.; Bode, H. B., Antiparasitic Chaiyaphumines from

Entomopathogenic Xenorhabdus sp. PB61.4. *J Nat Prod* **2014,** 27, 27.

9. Chae, C.; Kim, O.; Choi, C.; Min, K.; Cho, W. S.; Kim, J.; Tai, J. H., Prevalence of porcine epidemic diarrhoea virus and transmissible gastroenteritis virus infection in Korean pigs. *Vet Rec* **2000,** 147, (21), 606-8.

10. Zhang, J.; Fan, P.; Zhu, R.; Li, R.; Lin, Z.; Sun, B.; Zhang, C.; Zhou, J.; Lou, H., Marsupellins A-F, ent-Longipinane-Type Sesquiterpenoids from the Chinese Liverwort Marsupella alpine with Acetylcholinesterase Inhibitory Activity. *J Nat Prod* **2014,** 27, 27.

11. Ducatelle, R.; Coussement, W.; Pensaert, M. B.; Debouck, P.; Hoorens, J., In vivo morphogenesis of a new porcine enteric coronavirus, CV 777. *Arch Virol* **1981,** 68, (1), 35-44.

12. Pensaert, M. B.; de Bouck, P., A new coronavirus-like particle associated with diarrhea in swine. *Arch Virol* **1978,** 58, (3), 243-7.

13. Duarte, M.; Laude, H., Sequence of the spike protein of the porcine epidemic diarrhoea virus. *J Gen Virol* **1994,** 75, (Pt 5), 1195-200.

14. C. Bernasconi, F. G., A. Utiger, K. Van Reeth, M. Ackermann, A. Pospischil, *Clinical Histopathological and Immunohistochemical Findings* **1995**, 542–546.

15. K. Narayanan, S. M., in Nidoviruses ed. by Perlman, Snijder E.J., ASM Press, Washington, DC. **2008**, 235–244.

16. Chang, S. H.; Bae, J. L.; Kang, T. J.; Kim, J.; Chung, G. H.; Lim, C. W.; Laude, H.; Yang, M. S.; Jang, Y. S., Identification of the epitope region capable of inducing neutralizing antibodies against the porcine epidemic diarrhea virus. *Mol Cells* **2002,** 14, (2), 295-9.

17. Cruz, D. J.; Kim, C. J.; Shin, H. J., The GPRLQPY motif located at the carboxy-terminal of the spike protein induces antibodies that neutralize Porcine epidemic diarrhea virus. *Virus Res* **2008,** 132, (1-2), 192-6.

18. Godet, M.; Grosclaude, J.; Delmas, B.; Laude, H., Major receptor-binding and neutralization determinants are located within the same domain of the transmissible gastroenteritis virus (coronavirus) spike protein. *J Virol* **1994,** 68, (12), 8008-16.

19. Jackwood, M. W.; Hilt, D. A.; Callison, S. A.; Lee, C. W.; Plaza, H.; Wade, E., Spike glycoprotein cleavage recognition site analysis of infectious bronchitis virus. *Avian Dis* **2001,** 45, (2), 366-72.

20. Sturman, L. S.; Holmes, K. V., Proteolytic cleavage of peplomeric glycoprotein E2 of MHV yields two 90K subunits and activates cell fusion. *Adv Exp Med Biol* **1984,** 173, 25-35.

21. Sun, D.; Feng, L.; Shi, H.; Chen, J.; Cui, X.; Chen, H.; Liu, S.; Tong, Y.; Wang, Y.; Tong, G., Identification of two novel B cell epitopes on porcine epidemic diarrhea virus spike protein. *Vet Microbiol* **2008,** 131, (1-2), 73-81.

22. Bosch, B. J.; van der Zee, R.; de Haan, C. A.; Rottier, P. J., The coronavirus spike protein is a class I virus fusion protein: structural and functional characterization of the fusion core complex. *J Virol* **2003,** 77, (16), 8801-11.

23. Park, S. J.; Song, D. S.; Ha, G. W.; Park, B. K., Cloning and further sequence analysis of the spike gene of attenuated porcine epidemic diarrhea virus DR13. *Virus Genes* **2007,** 35, (1), 55-64.

24. Sato, T.; Takeyama, N.; Katsumata, A.; Tuchiya, K.; Kodama, T.; Kusanagi, K.,

Mutations in the spike gene of porcine epidemic diarrhea virus associated with growth adaptation in vitro and attenuation of virulence in vivo. *Virus Genes* **2011,** 43, (1), 72-8.

25. Utiger, A.; Tobler, K.; Bridgen, A.; Suter, M.; Singh, M.; Ackermann, M., Identification of proteins specified by porcine epidemic diarrhoea virus. *Adv Exp Med Biol* **1995,** 380, 287-90.

26. Nguyen, V. P.; Hogue, B. G., Protein interactions during coronavirus assembly. *J Virol* **1997,** 71, (12), 9278-84.

27. P.J.M. Rottier, in The Coronaviridae ed. by S.G. Siddel, Plenum Press, New York,. **1995**, 115–139.

28. L.J. Saif, Coronavirus immunogens. *Vet. Microbiol.* **1993**, 285–297.

29. Laude, H.; Gelfi, J.; Lavenant, L.; Charley, B., Single amino acid changes in the viral glycoprotein M affect induction of alpha interferon by the coronavirus transmissible gastroenteritis virus. *J Virol* **1992,** 66, (2), 743-9.

30. Baudoux, P.; Carrat, C.; Besnardeau, L.; Charley, B.; Laude, H., Coronavirus pseudoparticles formed with recombinant M and E proteins induce alpha interferon synthesis by leukocytes. *J Virol* **1998,** 72, (11), 8636-43.

31. Egberink, H. F.; Ederveen, J.; Callebaut, P.; Horzinek, M. C., Characterization of the structural proteins of porcine epizootic diarrhea virus, strain CV777. *Am J Vet Res* **1988,** 49, (8), 1320-4.

32. Curtis, K. M.; Yount, B.; Baric, R. S., Heterologous gene expression from transmissible gastroenteritis virus replicon particles. *J Virol* **2002,** 76, (3), 1422-34.

33. Schwarz, B.; Routledge, E.; Siddell, S. G., Murine coronavirus nonstructural protein ns2 is not essential for virus replication in transformed cells. *J Virol* **1990,** 64, (10), 4784-91.

34. Youn, S.; Leibowitz, J. L.; Collisson, E. W., In vitro assembled, recombinant infectious bronchitis viruses demonstrate that the 5a open reading frame is not essential for replication. *Virology* **2005,** 332, (1), 206-15.

35. Yount, B.; Roberts, R. S.; Sims, A. C.; Deming, D.; Frieman, M. B.; Sparks, J.; Denison, M. R.; Davis, N.; Baric, R. S., Severe acute respiratory syndrome coronavirus group-specific open reading frames encode nonessential functions for replication in cell cultures and mice. *J Virol* **2005,** 79, (23), 14909-22.

36. Song, D. S.; Yang, J. S.; Oh, J. S.; Han, J. H.; Park, B. K., Differentiation of a Vero cell adapted porcine epidemic diarrhea virus from Korean field strains by restriction fragment length polymorphism analysis of ORF 3. *Vaccine* **2003,** 21, (17-18), 1833-42.

37. Wood, E. N., Transmissible gastroenteritis and epidemic diarrhoea of pigs. *Br Vet J* **1979,** 135, (4), 305-14.

38. Pijpers, A.; van Nieuwstadt, A. P.; Terpstra, C.; Verheijden, J. H., Porcine epidemic diarrhoea virus as a cause of persistent diarrhoea in a herd of breeding and finishing pigs. *Vet Rec* **1993,** 132, (6), 129-31.

39. Kim, S. Y.; Song, D. S.; Park, B. K., Differential detection of transmissible gastroenteritis virus and porcine epidemic diarrhea virus by duplex RT-PCR. *J Vet Diagn Invest* **2001,** 13, (6), 516-20.

40. O. Kim, C. C., Can., Revue canadienne de recherche veterinaire. *J. Vet. Res.*

2002, 66, 112–116.

41. Y. Usami, O. Y., K. Kumanomido, Y. Matsumura, J., *Jpn. Vet. Med. Assoc.* **1998,** 51, 652–655.

42. Song, D. S.; Oh, J. S.; Kang, B. K.; Yang, J. S.; Moon, H. J.; Yoo, H. S.; Jang, Y. S.; Park, B. K., Oral efficacy of Vero cell attenuated porcine epidemic diarrhea virus DR13 strain. *Res Vet Sci* **2007,** 82, (1), 134-40.

43. Yuan, L.; Kang, S. Y.; Ward, L. A.; To, T. L.; Saif, L. J., Antibody-secreting cell responses and protective immunity assessed in gnotobiotic pigs inoculated orally or intramuscularly with inactivated human rotavirus. *J Virol* **1998,** 72, (1), 330-8.

44. Ward, L. A.; Yuan, L.; Rosen, B. I.; To, T. L.; Saif, L. J., Development of mucosal and systemic lymphoproliferative responses and protective immunity to human group A rotaviruses in a gnotobiotic pig model. *Clin Diagn Lab Immunol* **1996,** 3, (3), 342-50.

45. J., B., Medicinal Plants. Second Edition Hampshire UK, Intercept Ltd. *Phytochemistry* **1999**, 263-277.

46. Lacy, A.; O'Kennedy, R., Studies on coumarins and coumarin-related compounds to determine their therapeutic role in the treatment of cancer. *Curr Pharm Des* **2004,** 10, (30), 3797-811.

47. Venugopala, K. N.; Rashmi, V.; Odhav, B., Review on natural coumarin lead compounds for their pharmacological activity. *Biomed Res Int* **2013,** 963248, (10), 24.

48. Okuyama, E.; Hasegawa, T.; Matsushita, T.; Fujimoto, H.; Ishibashi, M.;

Yamazaki, M., Analgesic components of saposhnikovia root (Saposhnikovia divaricata). *CHEMICAL AND PHARMACEUTICAL BULLETIN-TOKYO-* **2001,** 49, (2), 154-160.

49. Hsu H.-Y., C. Y.-P., Shen S.-J., Hsu C.-S., Chen C.-C., Chang H.-; C., Oriental Materia Medica, a Concise Guide. In the Oriental Healing Arts Institute: Long Beach, California, U.S.A, 1986; 53-54.

50. Chen, I.-S.; Chang, C.-T.; Sheen, W.-S.; Teng, C.-M.; Tsai, I.-L.; Duh, C.-Y.; Ko, F.-N., Coumarins and antiplatelet aggregation constituents from formosan Peucedanum japonicum. *Phytochemistry* **1996,** 41, (2), 525-530.

51. Macias, F.; Massanet, G.; Rodr ́guez-Luis, F.; Salv á, J.; Fronczek, F., 13C NMR of coumarins. II—Khellactones: Spectroscopic criteria to establish the relative configuration of the dihydropyran ring. *Magnetic resonance in chemistry* **1989,** 27, (7), 653-658.

52. Matsuda, H.; Murakami, T.; Nishida, N.; Kageura, T.; Yoshikawa, M., Medicinal foodstuffs. XX. Vasorelaxant active constituents from the roots of Angelica furcijuga Kitagawa: structures of hyuganins A, B, C, and D. *Chemical & pharmaceutical bulletin* **2000,** 48, (10), 1429-1435.

6. Acknowledgement

Foremost, I am deeply grateful to my advisor, Prof. Choi Hong Seok and co-advisor, Prof. Oh Won Keun for the continuous support of my master's study and research. The guidance from professors helped me in all the time of research and writing of this thesis. I could not have imagined having better advisors for my master's study.

Besides my advisor, I would like to thank to our lab members Yang Jun-Li, Ha Thi Kim Quy, Kim Kuk Hwa and rest of the lab members for their continuous support and kind cooperation. Also, special thanks to former lab members, Sharma Govinda, Uddin Mohammad Nasir and Kim Ja Yeon.

I would also like to express my sincere gratitude to all professors and colleagues at College of Pharmacy, Chosun University as well as Seoul National University for their invaluable support and emotional encouragement during my graduate program.

Last but not the least; I would like to thank my parents (Narayan Dhodary and Rama Dhodary) and relatives for supporting me spiritually throughout my life.

Korea, May 2014

Basanta Dhodary